

UNCLASSIFIED

TEMPO  
C 9715  
Copy No. 114

DNA-TR-87-106

# CHARACTERIZATION OF DUST ENVIRONMENTS FOR THE F-107, TF-33, AND J-57 ENGINE TESTS (U)

P. J. Rausch, et al.  
R&D Associates  
P.O. Box 9695  
Marina del Rey, CA 90295

31 March 1988

Technical Report

CONTRACT No. DNA 001-85-C-0022

STATEMENT A  
Approved for public release;  
distribution is unlimited.

THIS WORK WAS SPONSORED BY THE DEFENSE NUCLEAR AGENCY  
UNDER RDT&E RMSS CODE B364079496 V99QAXNL12215 H2590D.

DECLASSIFIED WITH DELETIONS

Authority ED. 12526  
DTRA [Signature] Date 5/10/92

Prepared for  
Director  
DEFENSE NUCLEAR AGENCY  
Washington, DC 20305-1000

THIS DOCUMENT CONSISTS OF 86 PAGES,  
COPY 1 OF 1 COPIES, SERIES A.  
CLASSIFIED BY [Redacted] 1, dated August 1982.

Limitation to be inserted in this block by the originator. Do not insert "CONFIDENTIAL" or "SECRET" in this block.

UNCLASSIFIED

*Ad 01/16/88*

*[Redacted]*

*DNA 87 106 SAN*

*DNA 87 106 SAN*

From: Freeman, Betsy L. CIV  
Sent: Thursday, September 09, 2010 11:13 AM  
To: Lindsey, Robert H. MAJ USA  
Cc: Hoppe, Herbert CONTRACTOR; Cole, Richard M. CIV  
Subject: Fw: SAF/PA Case Completed: Case Number 2010-0507

Maj Lindsey,

Please forward this note to DTRIAC as official clearance from DTRA/PA that the AF/OSR clearance below has been verified and is final step in public release process. The documents should now be marked for Distribution A Public Release, Unlimited Distribution.

Thank you,  
Betsy Freeman  
Deputy Director  
Public Affairs  
Defense Threat Reduction Agency

----- Original Message -----

From: Devalee.Pridgen-Gattison@pentagon.af.mil  
<Devalee.Pridgen-Gattison@pentagon.af.mil>  
To: Freeman, Betsy L. CIV; dick.cole@dtra.mil <dick.cole@dtra.mil>  
Sent: Thu Sep 09 08:50:35 2010  
Subject: SAF/PA Case Completed: Case Number 2010-0507

SAF/PA has completed the review process for your case on 09 Sep 2010:

Subject: Report - Volcanic Ash Engine Data (Report)

Case Reviewer: Devalee Pridgen-Gattison  
Case Number: 2010-0507

The material was assigned a clearance of AF NO OBJECTION on 09 Sep 2010. If local policy permits, the Review Manager for your case, Devalee Pridgen-Gattison, Devalee.Pridgen-Gattison@pentagon.af.mil, will prepare a hard copy of the review and will forward it via mail or prepare it for pick up.

UNCLASSIFIED

SECURITY CLASSIFICATION OF THIS PAGE

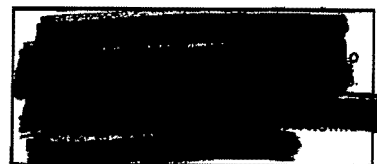
REPORT DOCUMENTATION PAGE				
1a. REPORT SECURITY CLASSIFICATION <del>SECRET</del>		1b. RESTRICTIVE MARKINGS <del>FORMERLY RESTRICTED DATA</del>		
2a. SECURITY CLASSIFICATION AUTHORITY CG-W-4, Rev. 1, dated August 1982.		3. DISTRIBUTION/AVAILABILITY OF STATEMENT A Approved for public release; distribution is unlimited.		
2b. DECLASSIFICATION/DOWNGRADING SCHEDULE N/A - None Formerly Restricted Data				
4. PERFORMING ORGANIZATION REPORT NUMBER(S) RDA-TR-135608-001		5. MONITORING ORGANIZATION REPORT NUMBER(S) DNA-TR-87-106		
6a. NAME OF PERFORMING ORGANIZATION R & D Associates	6b. OFFICE SYMBOL (If applicable)	7a. NAME OF MONITORING ORGANIZATION Director Defense Nuclear Agency		
6c. ADDRESS (City, State and ZIP Code) P.O. Box 9695 Marina del Rey, California 90295		7b. ADDRESS (City, State and ZIP Code) Washington, DC 20305-1000		
8a. NAME OF FUNDING/SPONSORING ORGANIZATION	8b. OFFICE SYMBOL (If applicable) SPWE/Adams	9. PROCUREMENT INSTRUMENT IDENTIFICATION NUMBER DNA 001-85-C-0022		
8c. ADDRESS (City, State and ZIP Code)		10. SOURCE OF FUNDING NUMBERS		
		PROGRAM ELEMENT NO. 62715H	PROJECT NO. V99QAXN	TASK NO. L WORK UNIT ACCESSION NO DH200900
11. TITLE (Include Security Classification) CHARACTERIZATION OF DUST ENVIRONMENTS FOR THE F-107, TF-33, AND J-57 ENGINE TESTS (U)				
12. PERSONAL AUTHOR(S) Rausch, P.J.; Yoon, B.L.; Greene, R.A.; Rawson, G.; and Mazzola, T.A.				
13a. TYPE OF REPORT Technical	13b. TIME COVERED FROM 821001 TO 871231	14. DATE OF REPORT (Year, Month, Day) 880331	15. PAGE COUNT 86	
16. SUPPLEMENTARY NOTATION This work was sponsored by the Defense Nuclear Agency under RDT&E RMSS Code B364079496 V99QAXNL12215 H25900.				
17. CREATI CODES		18. SUBJECT TERMS (Continue on reverse if necessary and identify by block number)		
FIELD	GROUP	SUB-GROUP		
4	2		Dust Environments	Classification
1	3		Dust Ingestion	Nuclear Dust Clouds
			Dust Cloud Modeling	Engine Tests
19. ABSTRACT (Continue on reverse if necessary and identify by block number) ✓ Environment limits are presented to guide a program for evaluating the potential hazards to turbojet aircraft engines from ingested dust generated during a nuclear exchange. Nuclear dust cloud environment limits are developed and used to define test conditions for specified engines on current strategic aircraft. The study emphasizes the glass component of the dust clouds. Estimates of particle size distribution are presented. Dust cloud characteristics (composition, size, stabilization altitude, and post-stabilization cloud movement) are discussed. Upper bounds on potential aircraft encounter conditions are defined for the ALCM F-107, TF-33, and J-57 engines, and testing conditions are suggested.				
20. DISTRIBUTION/AVAILABILITY OF ABSTRACT <input type="checkbox"/> UNCLASSIFIED/UNLIMITED <input type="checkbox"/> SAME AS RPT. <input type="checkbox"/> OTIC USERS		21. ABSTRACT SECURITY CLASSIFICATION UNCLASSIFIED		
22a. NAME OF RESPONSIBLE INDIVIDUAL Sandra E. Young		22b. TELEPHONE (Number Area Code) (202) 325-7042	22c. OFFICE SYMBOL DNA/CST!	

DD FORM 1473, 84 MAR

USE APR edition only to avoid conflict with automatic. All other editions are obsolete.

UNCLASSIFIED

SECURITY CLASSIFICATION OF THIS PAGE



[REDACTED]

UNCLASSIFIED

SECURITY CLASSIFICATION OF THIS PAGE

1. DISTRIBUTION/AVAILABILITY OF REPORT (Continued)

[REDACTED]

18. SUBJECT TERMS (Continued)

TF-33 Engine Tests  
F-107 Engine Tests  
J-57 Engine Tests

UNCLASSIFIED

SECURITY CLASSIFICATION OF THIS PAGE

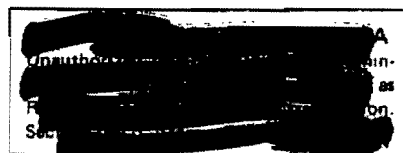
[REDACTED] to  
[REDACTED] ns  
[REDACTED] gn  
[REDACTED] nic

[REDACTED]

[REDACTED]

TABLE OF CONTENTS  
(This Table Is Unclassified)

Section		Page
	LIST OF ILLUSTRATIONS	iv
	LIST OF TABLES	v
1	INTRODUCTION	1
2	BACKGROUND	3
	2.1 The Problem	3
	2.2 Test Program Support	6
3	DUST CLOUD MODELING	9
	3.1 Quantity of Dust Lofted	12
	3.2 Cloud Stabilization Altitudes	15
	3.3 Particle Size Distribution	15
	3.4 Definition of Dust Quantities Considered	21
	3.5 Composition of the Lofted Dust	21
4	ESTIMATES OF DUST ENVIRONMENTS FOR ALCM FLY-IN	31
	4.1 Nuclear Attack Scenario	31
	4.2 Mission Profiles	34
	4.3 Dust Density Estimates	34
	4.4 Particle Size Range	43
	4.5 Soviet Soils: Dust Composition for the F-107 Tests	43
	4.6 Summary of Test Conditions	45
5	CONUS ENVIRONMENT	49
	5.1 Nuclear Attack Scenarios	49
	5.2 Mission Profiles	52
	5.3 Phenomenological and Modeling Uncertainties	58
	5.4 Results for PACCS and B-52s	62
	5.5 Radiation Exposure Constraints	67
	5.6 Summary of Test Conditions	71
6	LIST OF REFERENCES	75



# UNCLASSIFIED

## LIST OF ILLUSTRATIONS (This List Is Unclassified)

Figure		Page
1	Elements of the nuclear cloud model	10
2	Dust mass lofted into the stabilized cloud	13
3	Data base for lofted dust mass	14
4	Cloud stabilization heights--mid-latitude tests with yields >10KT	16
5	Particle size distribution in the stabilized cloud from a nuclear surface burst	18
6	Dust particle fall rates at 50 kft	20
7	Viscosities of important mineral and rock melts	25
<i>Deleted</i>	<del>8 Target locations in the modified scenario</del>	<del>33</del>
	9 Representative ALCM penetration flight paths	35
<i>Deleted</i>	<del>10 Dust environment near the ground--3 hours postattack</del>	<del>36</del>
<i>Deleted</i>	<del>11 Dust environment near the ground over western Soviet Union--3 hours postattack</del>	<del>38</del>
<i>Deleted</i>	<del>12 Dust environment near the ground over western Soviet Union--6 hours postattack</del>	<del>39</del>
<i>Deleted</i>	<del>13 Dust environment near the ground over western Soviet Union--10 hours postattack</del>	<del>40</del>
14	Dust encounter history along an example ALCM flight path	41
15	Dust density vs. duration of encounter	42
16	Particle size range near the ground	44
17	Suggested test envelope	46
18	Stabilized clouds from the modified PRIZE GAUNTLET scenario	51
19	Stabilized clouds from the alternative laydown on CONUS	54
20	Example of PACCS station areas	56
21	Hypothetical PACCS orbits covering CONUS	57
22	Hypothetical bomber flight paths	59
23	Nominal peak dust density vs. encounter duration for PACCS aircraft--early times	63

# UNCLASSIFIED

## LIST OF ILLUSTRATIONS (CONCLUDED)

(This List Is Unclassified)

Figure		Page
24	Nominal peak dust density vs. encounter duration for PACCS aircraft--late times	64
25	Peak density vs. encounter duration for bomber and tanker flyouts	66
26	Radiation levels vs. total intercepted dust mass for nominal PACCS environments	69
27	Radiation levels vs. peak dust density for nominal PACCS environments	70
28	Suggested test envelope--upper and lower bounds on the dust environment for PACCS aircraft	72
29	Particle size distribution of recommended CONUS environment composite	74

## LIST OF TABLES

(This List Is Unclassified)

Table		Page
1	Model inputs and outputs	22
2	Thermal properties and estimated weight percentages of dust-forming minerals	26
<i>Deleted</i> <del>3</del>	<del>Characteristics of the modified SABRE ENDURE scenario</del>	<del>32</del>
4	Suggested test materials	47
<i>Deleted</i> <del>5</del>	<del>Characteristics of the modified PRIZE GAUNTLET scenario</del>	<del>50</del>
6	Characteristics of the alternative laydown on CONUS	53
7	Summary of the parameter excursions and their impact on the resulting dust environment	60
8	Suggested screening and mixing specifications for CALSPAN (dust composite preparation for engine tests of the generic CONUS environment).	73

**UNCLASSIFIED**

THIS PAGE IS INTENTIONALLY LEFT BLANK.

vi

**UNCLASSIFIED**

# UNCLASSIFIED

## SECTION 1

### INTRODUCTION

(This Introduction Is Unclassified)

This report describes work performed by R & D Associates (RDA) in support of the Defense Nuclear Agency (DNA) program to evaluate the potential hazards to aircraft engines from dust clouds generated during a nuclear exchange. More specifically, this report summarizes our efforts to define engine test conditions representing bounds on the airborne dust environments that might be encountered by various military aircraft in the trans- and post-attack periods.

The DNA engine test program is being conducted in response to a 13 August 1983 letter from the Under Secretary of Defense for Research and Engineering (USDRE) requesting DNA's assistance in understanding levels of engine damage from dust ingestion. In part, this request was triggered by the catastrophic engine failures experienced during aircraft encounters with volcanic ash plumes.

**UNCLASSIFIED**

THIS PAGE IS INTENTIONALLY LEFT BLANK.

**UNCLASSIFIED<sup>2</sup>**

# UNCLASSIFIED

## SECTION 2

### BACKGROUND

(This Section Is Unclassified)

#### 2.1 THE PROBLEM.

It has long been recognized that dust lofted to aircraft operating altitudes either by nonnuclear means or by surface or near-surface nuclear explosions can cause damage to air-breathing engines. The damage mechanisms of most concern have included erosion of compressor components, reduced flow through turbine blade cooling passages, and contamination of lubrication systems.

Nearly catastrophic engine failures experienced during aircraft encounters with volcanic ash plumes (Refs. 1 and 2) demonstrated the existence of another, and possibly more serious, damage mechanism. Three such incidents are described briefly in the following paragraphs.

A Transamerica Hercules L-100 (C-130 equivalent) cargo aircraft, powered by four Allison T-56 turboprop engines, encountered the ash fall of the 25 May 1980 eruption of Mount St. Helens in Washington. The encounter occurred well below the main cloud about two hours after the eruption started; it lasted for three or four minutes. During this short exposure, the aircraft totally lost power on two engines and suffered temporary power losses in the other two. Inspection of the damaged engines showed abrasion of the compressor section and large amounts of glassy material coating the turbine section and temperature probes. It has been hypothesized that these deposits had two effects: (1) they formed over the thermocouple probes that are located just forward of the turbine inlet in the T-56 engine and disrupted the

## UNCLASSIFIED

fuel flow to the engine and (2) they formed in the turbine inlet itself and choked the flow into the turbine, causing the engines to surge. This damage is described in detail in Reference 1.

The next two incidents involved Boeing 747 aircraft. The first, on 24 June 1982, was a British Airways 747-236 powered by Rolls Royce RB-211 engines. At 37,000 ft, this aircraft entered a volcanic cloud resulting from the eruption of the volcano Galunggung near Jakarta, Indonesia. The aircraft lost thrust on all four engines, which were shut down for twelve minutes and subsequently restarted at about 12,000 ft when the aircraft exited the cloud.

In the second Galunggung incident on 13 July 1982, a Singapore Airlines 747 encountered a cloud of volcanic ash at 33,000 ft over Indonesia. Power was interrupted on three of the aircraft's four Pratt and Whitney JT9D-7A engines. One engine was restarted and a successful two-engine landing was accomplished at Jakarta. Inspection of the engines from both aircraft revealed heavy deposits on the turbine blades that appeared to be fused volcanic ash. Analyses of the material on the turbine blades of the Allison T-56 engines and the Rolls Royce RB-211 engines showed it to be primarily glass. Material deposited on the Pratt and Whitney JT9D-7A engines was not available for analysis.

Unlike other engine damage mechanisms known to be caused by dust, glassification (i.e., the deposition of glassy material on engine parts) involves a thermodynamic interaction between the hot section of the engine and the ingested dust. As hypothesized, the mechanism begins with the melting or softening of the glassy dust material as it passes through

## UNCLASSIFIED

the engine's combustors, followed by deposition of glassy deposits on downstream metal surfaces, especially in the vicinity of the turbine inlet. How important glassification is depends on the temperature at which the dust material softens to the point of being tacky and capable of sticking to the surfaces. Since natural glass is the constituent of volcanic dust that will soften and become tacky at the lowest temperature, it is hypothesized that the glassification potential of dust depends largely on its glass fraction.

Concern has been expressed that glassification also may result when an aircraft penetrates the dust clouds that would be lofted by surface or near-surface detonation of nuclear weapons, because such detonations do form a certain amount of glass. The principal mechanism for formation of this glass is the heating of the lofted dust as it passes through the fireball. Glass so formed is expected to be concentrated in the smaller particles and therefore would be lofted into the high-altitude dust cloud, where it could remain for an extended period.

Since the glass produced by nuclear surface bursts should have softening temperatures similar to those of the glass in volcanic ash, particulate matter lofted by such nuclear explosions could produce glassy aircraft-engine deposits similar to those caused by the volcanic ash. As in the three volcanic ash encounters, this glassification could choke the flow through the engine, leading to flow instability (surge), or could cause engine sensor malfunctions. If this is shown to be true, it would have serious implications for the operation of strategic aircraft in the critical time period immediately following a large-scale missile exchange.

# UNCLASSIFIED

In summary, the engine damage that has been observed to result from aircraft encounters with volcanic dust clouds suggests that glassification, which was not previously thought to be important, could have catastrophic consequences for aircraft that penetrate nuclear dust clouds. The estimates of nuclear dust cloud environments that are presented in this report will establish environmental conditions for an engine test program to investigate this potential problem.

## 2.2 TEST PROGRAM SUPPORT.

The primary objectives of the DNA engine test program are to (1) determine the tolerance of aircraft turbine engines to dust ingestion, (2) determine whether glassification would cause catastrophic damage in realistic worst-case scenarios, and (3) provide a quantitative understanding of the glassification damage mechanism. In response to the USDRE directive cited, the initial phases of this test program address damage to engines currently used on strategic aircraft.

As part of the early test planning, RDA identified and assigned priorities to a spectrum of missions for strategic aircraft and the engines potentially at risk and outlined recommendations for the test program (Ref. 3). These missions include

- U.S. bomber and cruise missile penetration of the Soviet Union following an exchange of strategic missiles between the two countries.
- U.S. bomber and tanker egress from CONUS and C<sup>3</sup> aircraft operations in the United States, following such an exchange.

# UNCLASSIFIED

The engines from the currently operational strategic aircraft that are being tested in the program's first phase are the ALCM F-107 engine and the TF-33 and J-57 engines on the B-52, KC-135, and Post-Attack Command and Control System (PACCS) aircraft. The tests are being performed by the Arvin/Calspan Corporation in Buffalo, New York.

To provide a basis for establishing conditions to test these engines, RDA estimated upper bounds on the environments that would be generated by hypothetical nuclear laydowns. These environments were characterized in terms of dust density, particle size, glass fraction, and mineralogical properties.

A major difference between the suggested test conditions resulting from the analyses and those used in previous engine tests is the dust composition. Previous tests focused on erosion damage caused by dust ingestion. The dust composition was therefore chosen to emphasize erosive qualities. The estimated dust environments described in this report were composed to place more emphasis on the glass fraction, and therefore to attempt a better balance between erosion and glassification based on what might be expected to be the composition of dust clouds lofted by surface nuclear explosions. The importance of the various mechanisms is to be determined by engine testing.

The following sections describe our results and the supporting analyses. Section 3 summarizes our modeling efforts, discusses the impact of selected uncertainties in the phenomenology, and describes key properties of materials lofted by near-surface bursts. Section 4 presents the estimates of dust density and particle size that were used to guide test conditions for the ALCM F-107 engine. These

## **UNCLASSIFIED**

estimates were based on a hypothetical counterforce laydown on the Soviet Union. Section 5 presents similar estimates that were used to guide test conditions for the TF-33 and J-57 engines. For these estimates, two hypothetical Soviet counterforce laydowns on the United States were considered. Sections 4 and 5 are presented as independent studies, each with its own conclusions.

# UNCLASSIFIED

## SECTION 3

### DUST CLOUD MODELING

(This Section Is Unclassified)

To characterize dust environments that could be produced by a nuclear attack, RDA has developed a computer model to predict airborne dust densities at specified altitudes. The model currently describes only the airborne cloud and its particle fallout; it does not treat the dust stem or the dust pedestal.\*

As shown in Figure 1, the model starts with an empirical description of the stabilized dust clouds based on available nuclear test data, all at mid-latitudes. Stabilization is defined as the time at which cloud rise ceases. Stabilization times range from three to fifteen minutes, depending on yield, local meteorology, and tropopause altitude variations with latitude.

After the cloud stabilizes, its motion is governed primarily by ambient atmospheric dynamics. The model treats the cloud's dynamics as advective-diffusive transport with gravitational sedimentation. It computes cloud transport by ambient winds, cloud spread based on a turbulent diffusion description, and particle settling based on equations for spherical particles falling through still air. Parameters in the dynamics equations were derived using data from nuclear tests, high-

---

\* For megaton yields, the high-altitude cloud is expected to be the dominant source of dust at aircraft operating altitudes over CONUS. The dust stem is considerably smaller and at a lower altitude. On the other hand, the dust pedestal could be a significant dust source during aircraft takeoff or during low-altitude penetration over the Soviet Union. We have attempted to account for its effects in estimating upper bounds on environments.

# UNCLASSIFIED

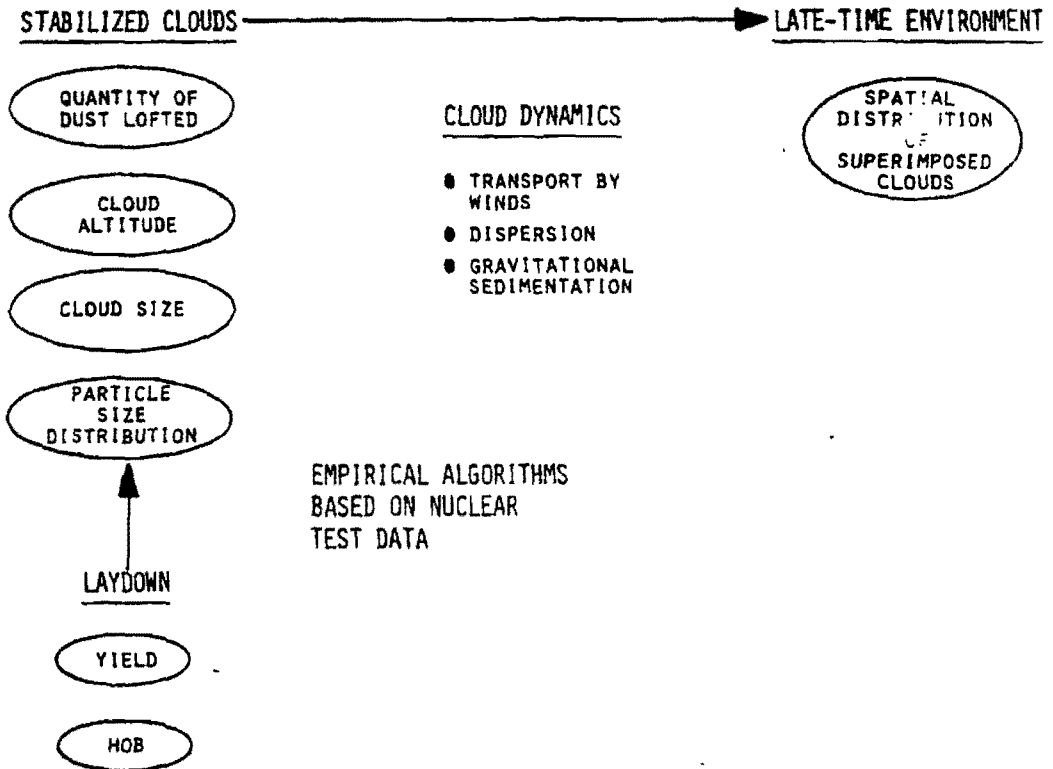


Figure 1. Elements of the nuclear cloud model.

# UNCLASSIFIED

explosive tests, naturally occurring relevant phenomena such as the observed behavior of volcanic dust plumes, and hydrocode results.

The details of the model and the phenomenology that it embodies are described more fully in Reference 4. We highlight here some of the parameters that are considered particularly important in determining the dust environments in which aircraft might have to operate:

- Quantity of dust lofted
- Cloud stabilization altitudes
- Particle size distribution in the stabilized cloud
- Mineralogy of the lofted particles

It should be emphasized that the following descriptions of dust cloud parameters are characterized by substantial uncertainties. These uncertainties arise from limitations both in the nuclear test data base and in our understanding of nuclear burst phenomenology. Principally, these uncertainties arise because all of the U.S. nuclear tests conducted over continental soils used very low yield detonations (<1-KT surface bursts, <70-KT nonsurface bursts) and only a few of them could be classified as surface or near-surface bursts. Furthermore, there were a limited number of measurements from which dust cloud characteristics could be inferred.

In addition to the limitations in the nuclear test data base, other aspects of the phenomenology are poorly understood and are therefore either not represented or only approximately represented in our model. These include the effects of multiple bursts, meteorological conditions, lofted water vapor, particle agglomeration, and soil geology.

# UNCLASSIFIED

For the case of multiple burst interactions, lacking sufficient information to quantify their effects, we treated each burst in the laydowns used in this study as a single, independent entity, and superposed the resulting high-altitude clouds to determine total dust densities. Recent hydrocode calculations indicate that nearly simultaneous, closely spaced megaton-class bursts may lead to an increase in stabilization altitudes of about 20 percent. However, these are preliminary results. Moreover, they do not address the interactions of moderately spaced bursts, such as those characteristic of missile silo spacings.

Also, very recent, preliminary hydrocode runs done by Rosenblatt (of California Research & Technology, Inc.) indicate that the dust pedestal may be the dominant source of dust at low altitudes and that the dust levels can be significant for post-detonation times of several to tens of hours.

## 3.1 QUANTITY OF DUST LOFTED.

The severity of the dust environment encountered by aircraft depends on the quantity of dust lofted by the nuclear explosion. Figure 2 shows our estimate of the amount of dust lofted into the stabilized cloud as a function of yield and height of burst (Refs. 5 and 6). As shown in the figure, the mass loading for surface bursts is nominally estimated to be 0.3 MT of dust per megaton of weapon yield. The figure shows that the uncertainty bounds estimated in Reference 5 are a factor of approximately 3 higher or lower than the nominal values.\* Figure 3 (summarized from Ref. 7) shows some of

---

\* Some researchers feel that the uncertainty bound (particularly for surface bursts) is smaller than the factor of 3 indicated above.

# UNCLASSIFIED

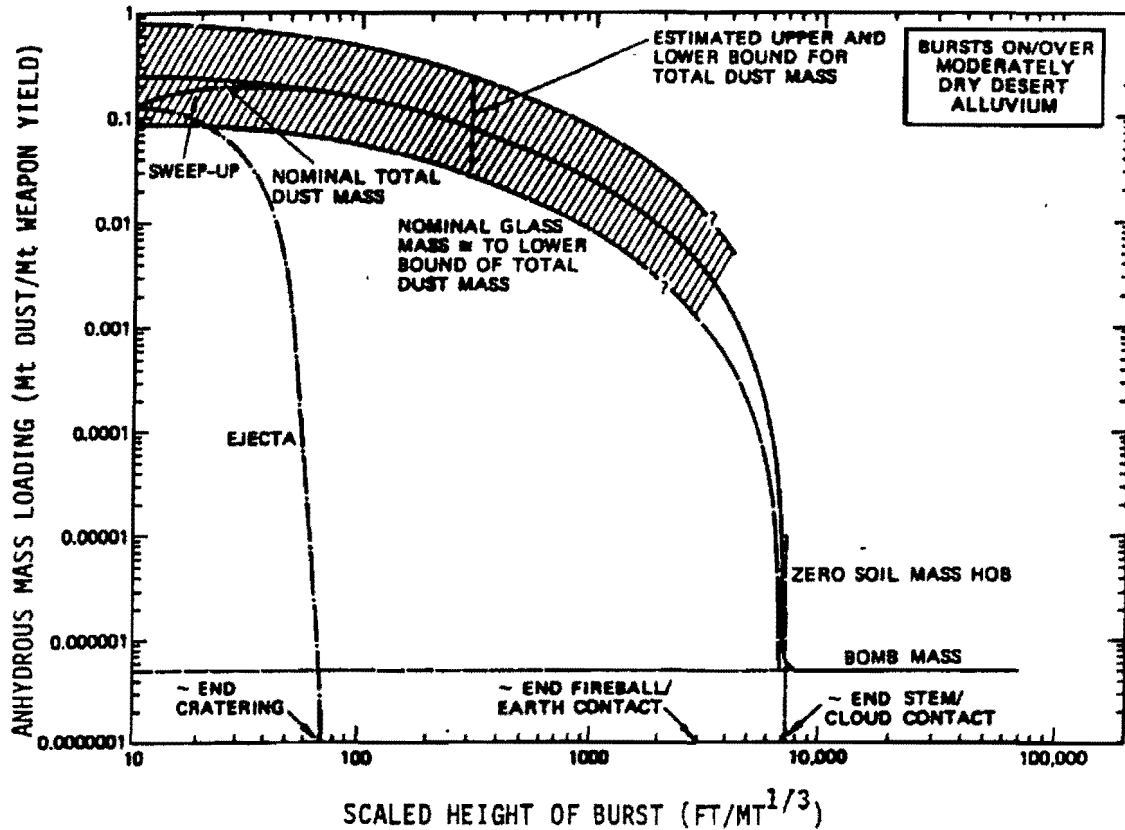


Figure 2. Dust mass lofted into the stabilized cloud.

# UNCLASSIFIED

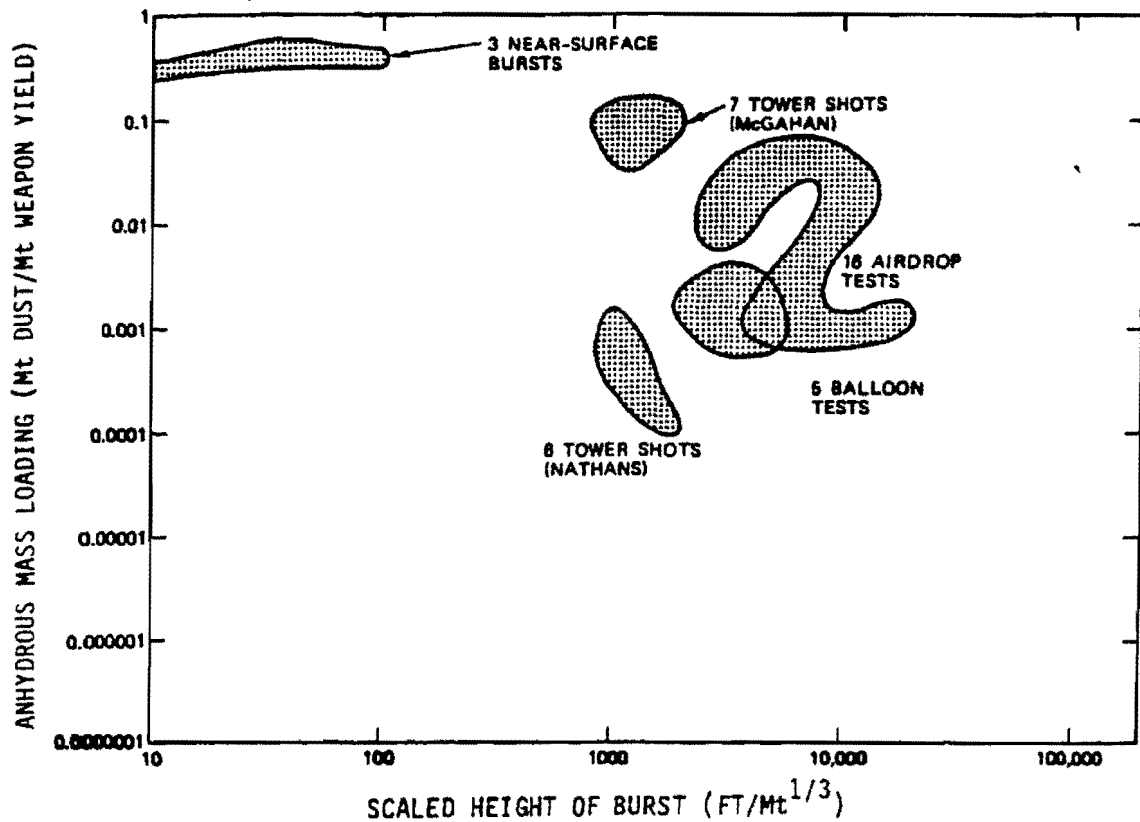


Figure 3. Data base for lofted dust mass.

# UNCLASSIFIED

the derived data on which Figure 2 is based. It includes a selection of nuclear tests over continental soils. The mass loading estimates were inferred from radiochemical analyses and beta radioactivity measurements made on cloud and fallout samples.\*

## 3.2 CLOUD STABILIZATION ALTITUDES.

Since dust densities are higher within the main cloud layer than below it, aircraft environments are sensitive to the base altitude of the stabilized cloud. The average base altitude and vertical extent of the stabilized cloud at mid to polar latitudes is shown in Figure 4. The cloud height curves were fitted to the observed dimensions of the visible clouds from U.S. and selected foreign nuclear tests at mid-latitudes (Refs. 8 and 9). These visible cloud data were obtained over a range of seasons and meteorological conditions. For isolated bursts and seasonally averaged meteorological conditions, the cloud from a 1-MT surface burst is predicted to extend from about 35 to 55 kft. However, as meteorological conditions vary, these altitudes may vary as much as 10 kft in either direction. Such variations in cloud stabilization altitudes could be particularly significant for trans- and post-attack aircraft operations over CONUS.

## 3.3 PARTICLE SIZE DISTRIBUTION.

Since fall rates vary with particle size, the distribution of particle sizes affects the relative proportion of dust in and

---

\* DNA is currently sponsoring a program to improve the data base on stabilized cloud characteristics. The work includes estimates of mass loadings from previously unanalyzed cloud samples from foreign nuclear tests.

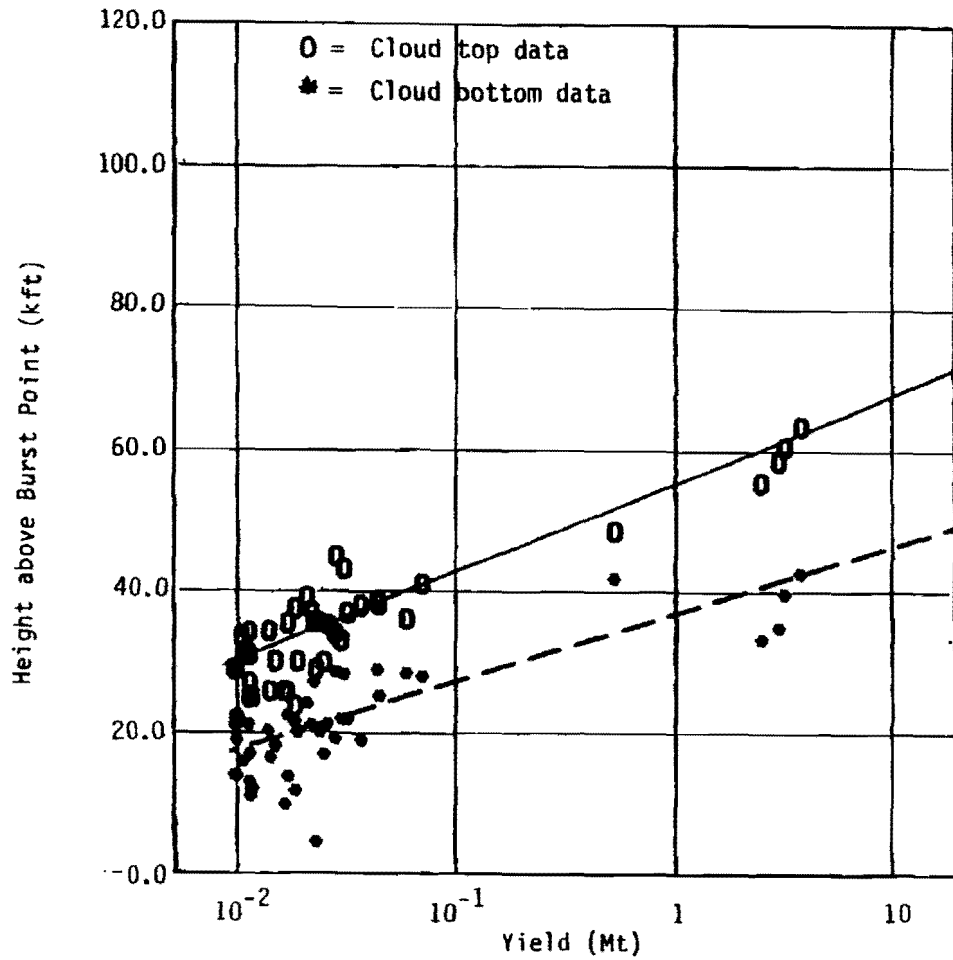


Figure 4. Cloud stabilization heights-- mid-latitude tests with yields >10KT.

# UNCLASSIFIED

below the main cloud layer or, more generally, the distribution of dust mass with altitude. The size of the particles entering an engine's combustor also affects the particles' melting rates and their subsequent flow trajectories through the aircraft engine. Although the size of the particles entering the combustor was expected to depend on the particle sizes entering the compressor section of the engine, there is some early test evidence from this program that the dust particles are broken up and reduced in size as they pass through the compressor. This evidence suggests that the particles exiting the compressor are less than 10  $\mu\text{m}$  in diameter, independent of the particle sizes that originally entered the engine. However, this needs to be confirmed by further testing.

Figure 5 shows estimates of particle size distributions that might initially exist within the stabilized cloud. We based our nominal estimate on analyses of a cloud sample from the 0.5-KT JOHNNIE BOY nuclear test (July 1962), which was detonated slightly below the surface in Nevada.\* This burst is the only nuclear test involving continental soil for which detailed particle size data have been collected and analyzed (Ref. 10).\*\* The solid line on the JOHNNIE BOY curve indicates the range of sizes for which data exist. We extrapolated this curve (dotted lines) so that particle size would

---

\* The particle size distribution probably depends on a number of factors specific to the detonation (e.g., yield, height of burst) and to the soil and terrain (e.g., soil properties, moisture content, topography, vegetation). However, there are insufficient data to quantify the influence of these factors.

\*\* Some data and samples exist from other surface bursts over soil but have not yet been analyzed.

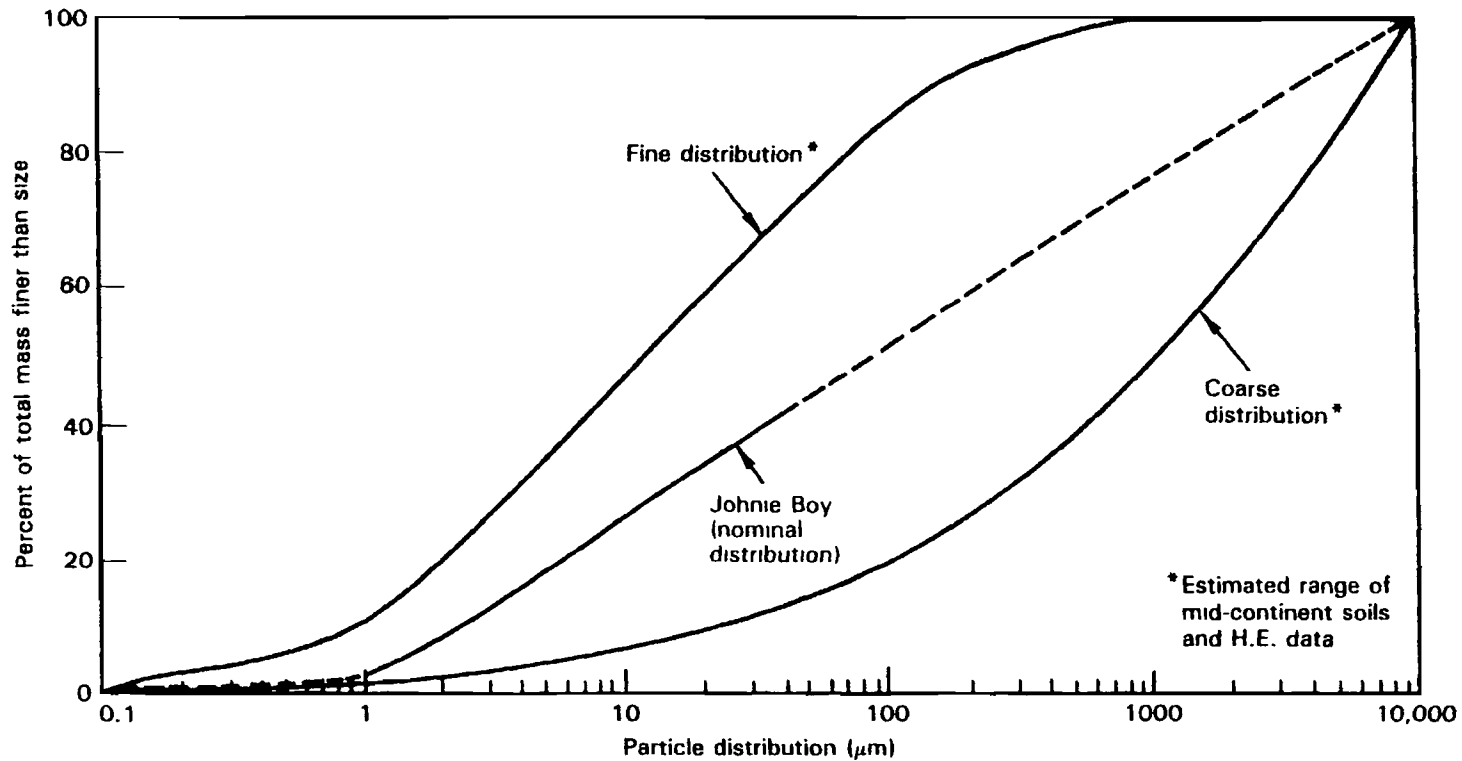


Figure 5. Particle size distribution in the stabilized cloud from a nuclear surface burst.

## UNCLASSIFIED

cover the range from 0.1  $\mu\text{m}$  to 1 cm. Particles within this size range are estimated to be present in the stabilized (i.e., approximately ten-minute-old) cloud from a 1-MT surface burst over midcontinental soil. The outer lines of Figure 5 show preliminary estimates of the possible range of variability based on analyses of ambient soils lofted by high explosives (HE).

We assumed the particle size distribution to be uniform throughout the spatial extent of the visible stabilized cloud.\* At times after stabilization, the particle sizes are redistributed spatially by gravitational sedimentation. For mid-latitude clouds, Figure 6 shows particle fall rates at 50 kft and total fall times from that altitude.

As indicated, particles larger than 1 mm (which account for about 25 percent of the lofted dust mass) have reached the ground after about 25 minutes.

The particle size range that an aircraft is predicted to encounter depends on both the flight altitude relative to initial stabilized cloud layers and the time that has elapsed since the explosion. For the post-laydown times of interest and the scenarios we considered, using the JOHNIE BOY distribution, the maximum particle diameter encountered is typically on the order of 200 to 300  $\mu\text{m}$ . To facilitate the production of soil mixtures for the engine tests, we assumed a nominal maximum size of 250  $\mu\text{m}$  for clouds at least one-half hour old.

---

\* Various models predict vertical stratification of particle sizes in the stabilized cloud, with larger particles concentrated near the cloud bottom. However, the results of this study are relatively insensitive to the initial degree of vertical stratification.

# UNCLASSIFIED

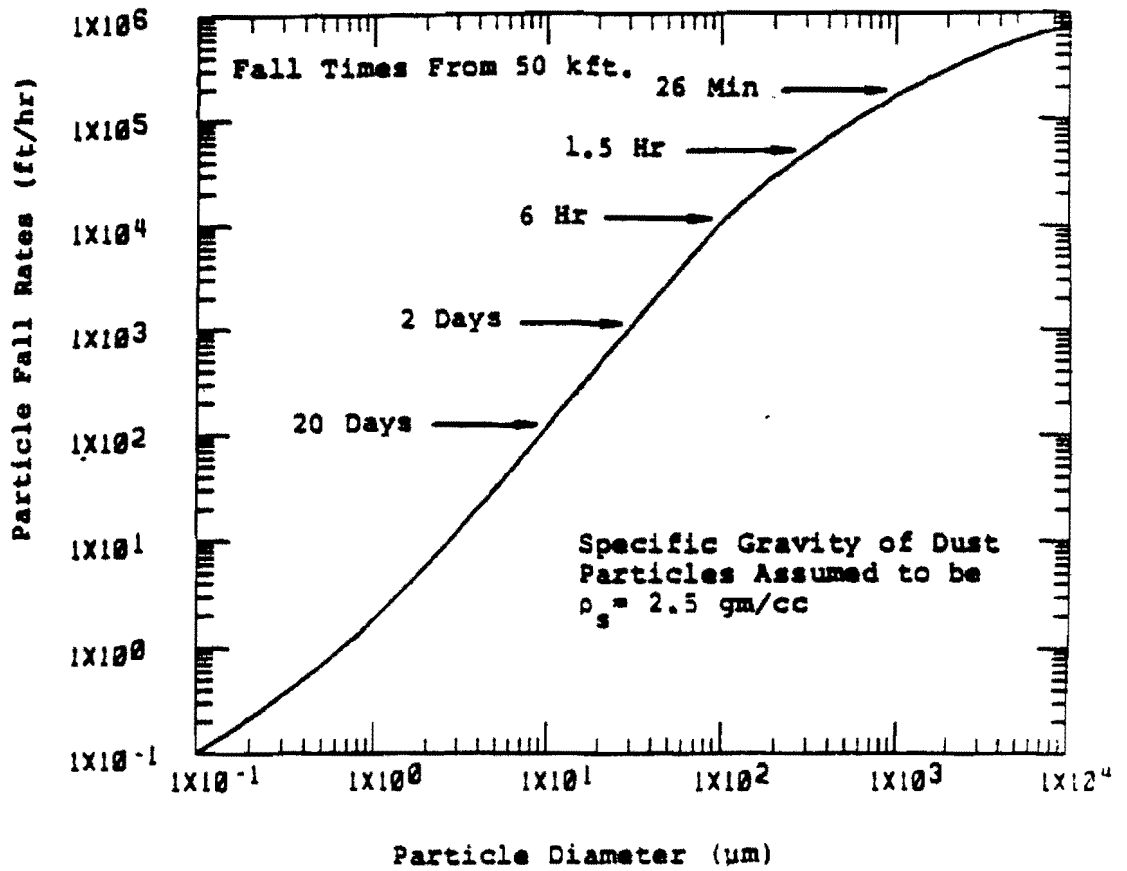


Figure 6. Dust particle fall rates at 50 kft.

# UNCLASSIFIED

## 3.4 DEFINITION OF DUST QUANTITIES CONSIDERED.

Table 1 summarizes the major input parameters required by our dust cloud model. The table also lists the model outputs. The outputs include the density,  $\rho$ , of the dust in the air that is encountered by the aircraft as a function of time; ingested mass of dust as a function of time; and the total mass,  $M_t$ , of dust ingested over a specified time interval. Postprocessor programs use these quantities to define for a specific flight profile the peak dust density encountered,  $\rho_p$ , the ingestion rates, and a characteristic ingestion time,  $T$ , which is defined such that  $M_t = \rho_p v T$ , where  $v$  is the aircraft velocity.

## 3.5 COMPOSITION OF THE LOFTED DUST.

The focus of this study is the definition of bounding conditions to be used in tests to study turbine engine damage caused by dust ingestion--especially through the process of glassification. In this section we will discuss the composition of dust materials that might be expected to cause glassification if they were to be ingested by a turbine engine. For the reasons given in Section 3.5.1, a very important feature of the dust's composition is its glass fraction. Properties of glass made from commonly occurring minerals are discussed in Section 3.5.2 and the glass content of dust clouds that would be caused by nuclear surface bursts in Section 3.5.3.

Even though we have emphasized the glass fraction in defining dust compositions, we have included in recommended test mixtures the appropriate other common soil and rock minerals. This gives a reasonable balance between the erosion and

# UNCLASSIFIED

Table 1. Model inputs and outputs.

Model inputs	Model outputs
● Laydown	● Dust densities encountered (mg/m <sup>3</sup> )
● Stabilized cloud parameters - dust loading factors - cloud stabilization altitudes - particle size distribution	● Dust ingestion rates (g/m <sup>2</sup> -s)
● Winds	● Total mass ingested (kg/m <sup>2</sup> )
● Aircraft mission profiles - flight path/orbit areas - cloud entry time	● Maximum particle size encountered
● Cell size - vertical - horizontal	

## UNCLASSIFIED

glassification potentials of the dust used in the engine tests.

### 3.5.1 Importance of the Glass Fraction.

It has been postulated that glassification is caused by glass in a heated, tacky state adhering to hot engine sections, such as nozzle guide vanes or thermocouple probes. The reason the glass might be tacky when it arrives at the turbine face is obvious--it is still hot from its passage through the combustor. However, the most likely origin of the glass that would form these deposits is not so obvious. Soils commonly contain only one or two percent glass, which is probably not enough to cause a problem. Thus, for glassification to occur requires that additional glass be made by melting some of the silicates present in crystalline form in the soil.

There are at least two possible processes through which this additional glass could be made: (1) It could be formed by the melting or vaporizing of crystalline dust particles during passage through the fireball as the dust is being lofted into the stabilized cloud, in which case it would be present in the dust ingested by the engine; or (2) it could be formed as the crystalline dust particles pass through the engine's combustor.

We have emphasized the first of these processes for two reasons. First, a significant amount of the dust lofted by a surface burst would pass through the fireball and turn into glass (through the process described in Section 3.5.3); so whether additional glass is made in the engine's combustor is of secondary importance. Second, the conditions required to melt crystalline materials and convert them to glass may be

# UNCLASSIFIED

more difficult to attain than those required to make glass tacky. The stoichiometric combustor temperatures may be high enough to melt the crystalline materials if they are exposed long enough. However, how much glass would be formed in a combustor depends on such parameters as the particle size, the residence time, and the degree of thermal equilibrium between the airstream and the dust itself.

## 3.5.2 Physical Properties.

Figure 7 displays the calculated temperature dependence of the viscosity and the melting points of the amorphous, or glass, form of several minerals that are characteristic of midcontinental soils (Ref. 11). Note first that quartz represents an upper bounding material and that its melting point (about 1700 C) is well above those of the other materials.

Note further that glasses formed from the feldspars albite and anorthite represent upper and lower bounds for the viscosities of most silicate minerals other than quartz. This is significant since, other than quartz and clay (Table 2), feldspars are the major components of the three most common near-surface rocks of the earth's crust: granite, shale, and basalt. Most soils are derived from these sources (Ref. 13). Viscosities of glasses made from granitic materials are toward the upper side of the band shown, whereas those of shale and basaltic glasses are toward the bottom of the band.

Calculated curves for two glasses are also shown--Mount St. Helens ash and Twin Mountain scoria. The Mount St. Helens glass was extracted from samples of the 18 May eruption. The scoria is another form of natural glass. The turbine inlet temperature (TIT) for the T-56 engine is noted on the Mount

# UNCLASSIFIED

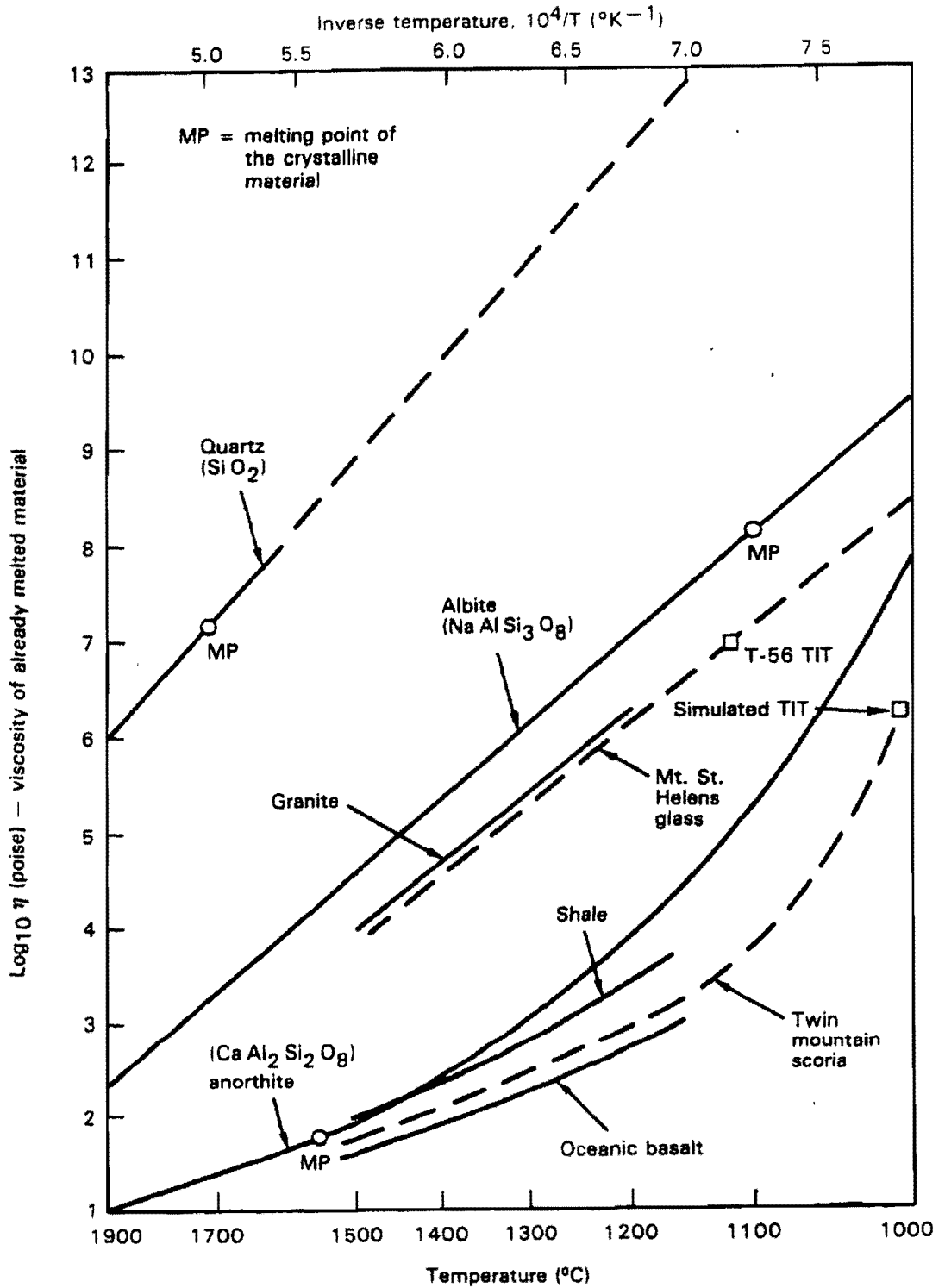


Figure 7. Viscosities of important mineral and rock melts.

# UNCLASSIFIED

Table 2. Thermal properties and estimated weight percentages of dust-forming minerals.

Mineral	Fusion, °C (dissociation)	Global Average Sediments (%)
Quartz	1713	38
Feldspars and Mica	1100 to 1551	17
Albite	1100	(specified as
Anorthite	1551	feldspar)
Clay Minerals	(900 to 1400)	24
Calcite and dolomite	(800 to 900)	14
Gypsum	(1050)	2
Accessory minerals	1200 to 1700	5
Glass	700 to 1150*	1

\*Estimated threshold of fusion; brittle-tacky transition.

# UNCLASSIFIED

St. Helens glass curve, since that encounter produced glassification.

It is postulated that the glassification process is characterized by a threshold value of the viscosity of the glass melt entering the engine turbine section. This suggests that the turbine inlet temperature is a significant glassification parameter. Such a conclusion is reasonable, assuming the dust particle surfaces to be in thermal equilibrium with the surrounding hot gases, since this temperature would characterize the thermodynamic state of the dust particle surface at the point in the engine where the glassy deposits have been observed.

Characterizing the glassification potential of a given situation by the turbine inlet temperature has the additional virtue that it is a commonly available engine quantity.\*

### 3.5.3 Glass Fractions in the Lofted Dust.

As noted, there have been no direct measurements of the glass fraction in dust samples from surface or near-surface nuclear detonations, since the glass content of lofted dust was not previously thought to be important. The estimates presented in this section are therefore based on available data from existing DICE-code calculations. DICE is a computer program

---

\* Noted on the Twin Mountain scoria curve is the simulated inlet temperature at which glassification occurred in a laboratory simulation test. The fact that (within the accuracy of these calculated characteristic curves) glassification in both these situations occurred at about the same viscosity ( $10^6$  to  $10^7$  poise) supports (or at least does not contradict) our postulate that the dust's viscosity may characterize the glassification process.

## UNCLASSIFIED

developed by California Research and Technology (CRT). DICE-code calculations are used because they represent DNA's best model for the interaction of crater ejecta and swept-up dust with the nuclear fireball, the primary source of glass production.\* Although these calculations model the momentum and energy interchange between the hot gases and groups of various sizes of dust particles, they do not provide for careful attention to details of the particulate phase change. Nevertheless, they do provide us with a rough estimate of the dust mass that has been melted or vaporized.

The melt criterion used was a specific internal energy of  $1.7 \times 10^{10}$  ergs/gm, or about  $1700^{\circ}\text{C}$ . Vaporization temperature is a function of pressure but is about  $2200^{\circ}\text{C}$  at one atmosphere.

The most recent surface-burst dust cloud calculation with the DICE code is N-3. It is a 100-KT surface burst calculation (Ref. 14). The total dust mass aloft (above one kilometer) at ten minutes after burst is 25 KT, or 0.25 KT of dust per kiloton of yield. The amount of dust melted or vaporized is not monitored during the calculation. Also, in the version of DICE used for N-3, particles were not allowed to fall out, so the percentage of larger particles is higher than it should be. However, CRT was able to recover some of the relevant information from restart tapes. In particular, CRT was able to determine the maximum instantaneous amount of material in the vapor and liquid phases. These values are 1.75 KT of dust vapor at 0.34 s and 1.6 KT of liquid dust particles at 1.5 s (Ref. 15).

---

\* A cursory review of another calculation, the S-CUBED BM-3 early-time deposition calculation, indicated that less than one percent of the lofted dust is melted by the initial bomb energy deposition in the ground (Ref. 13).

## UNCLASSIFIED

The peak instantaneous values are a lower bound to the total mass that is passed through each state, since there is some additional mass that has already passed or will yet pass through either state. From a previous calculation, DICE case 708 (Ref. 16), it was found that the total recondensed dirt vapor mass is about twice the peak instantaneous value. This factor suggests a total condensed vapor mass of 3.5 KT for case N-3, or 3.5 percent of the yield. This value compares reasonably well with the range of values, 1.5 to 4 percent, obtained from Reference 15 for a series of four calculations.

The value of 3.5 KT is an estimate for the glass content of the newly formed stabilized cloud. Such a cloud would contain large particles that would be immediately hazardous to the aircraft's airframe and the cloud would also be rather small at this time. For these reasons it has been assumed that the clouds of interest for establishing engine test conditions are at least half an hour old and comprise particles with diameters of 250  $\mu\text{m}$  or smaller. On the basis of the initial dust particle size distribution, particles smaller than 250  $\mu\text{m}$  represent about 40 percent of the cumulative mass up to approximately 1 cm (which is the largest size still aloft at ten minutes). The estimate for total mass aloft at the later time is then approximately 10 KT. The glass fraction at this time is thus about one third to one half, if we assume that all of the glassified material has particle diameters less than 250  $\mu\text{m}$ . This seems reasonable, since smaller particles interact thermally and are therefore melted more readily owing to their larger ratios of surface area to mass. Furthermore, the glass fraction may continue to increase with time as the larger, less glassy particles fall out.

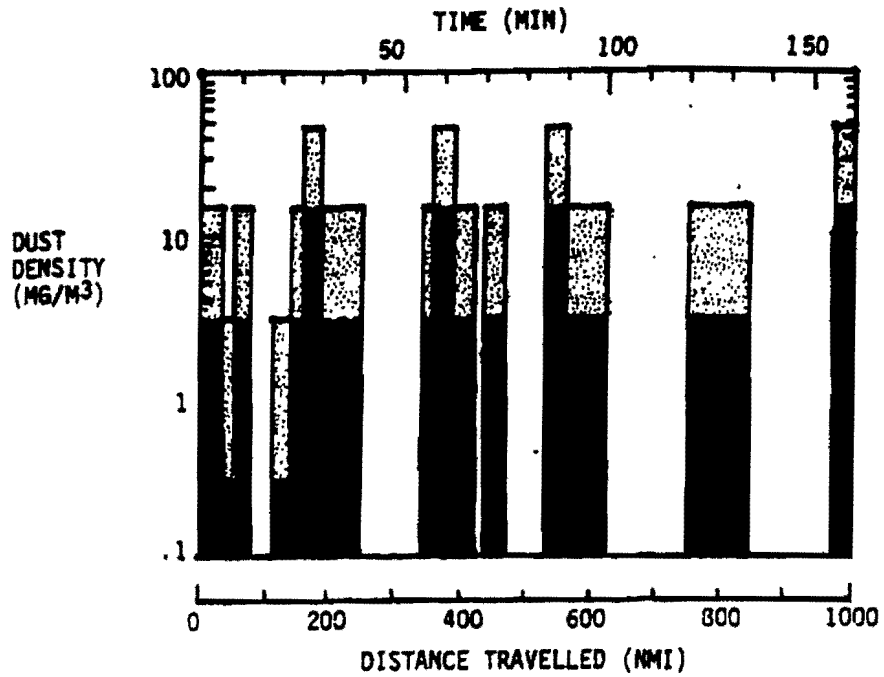
UNCLASSIFIED

## UNCLASSIFIED

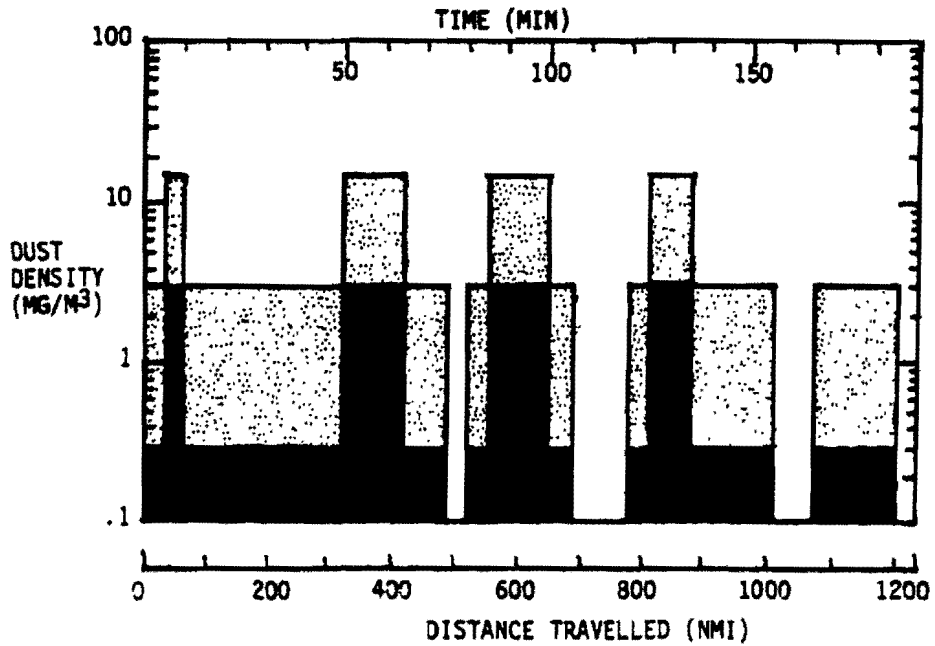
Two factors that could affect this estimate were not considered. The first is the amount of mass that is melted and converted to glass but never vaporized. At the present time there is no way to retrieve this information from the existing calculations. Its effect would be to increase the glass fraction. The second factor is the dilution of the glass fraction that would occur if more dust were contained in the stabilized cloud than the 25 KT per 100 KT of weapon yield predicted in this DICE run. In comparison, the lofting efficiency used in estimating the amount of dust that might be encountered by an aircraft in flight, as described in Sections 4 and 5, is between 0.1 and 1.0 MT of dust in the stabilized cloud per megaton of yield.

In summary, the best and most reasonable estimate that can be made on the basis of the existing dust cloud calculations is a glass fraction of one third to one half for a surface-burst dust cloud, at times ranging from a half hour to one hour.

UNCLASSIFIED



a. (U) Dust environment at 3 hours.



b. (U) Dust environment at 10 hours.

UNCLASSIFIED

Figure 14. (U) Dust encounter history along an example ALCM flight path.

UNCLASSIFIED

# UNCLASSIFIED

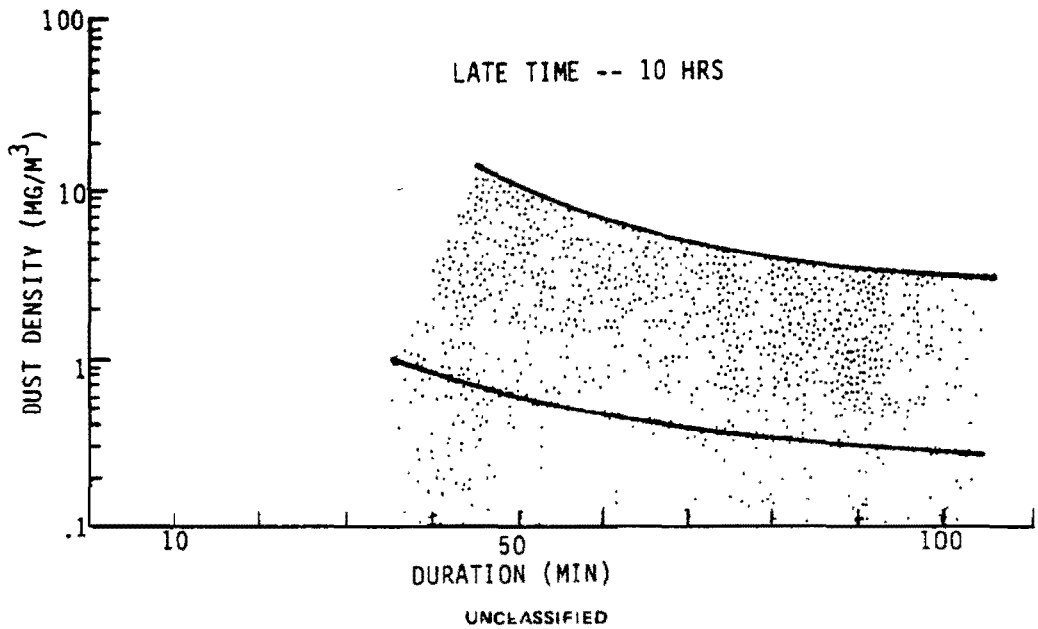
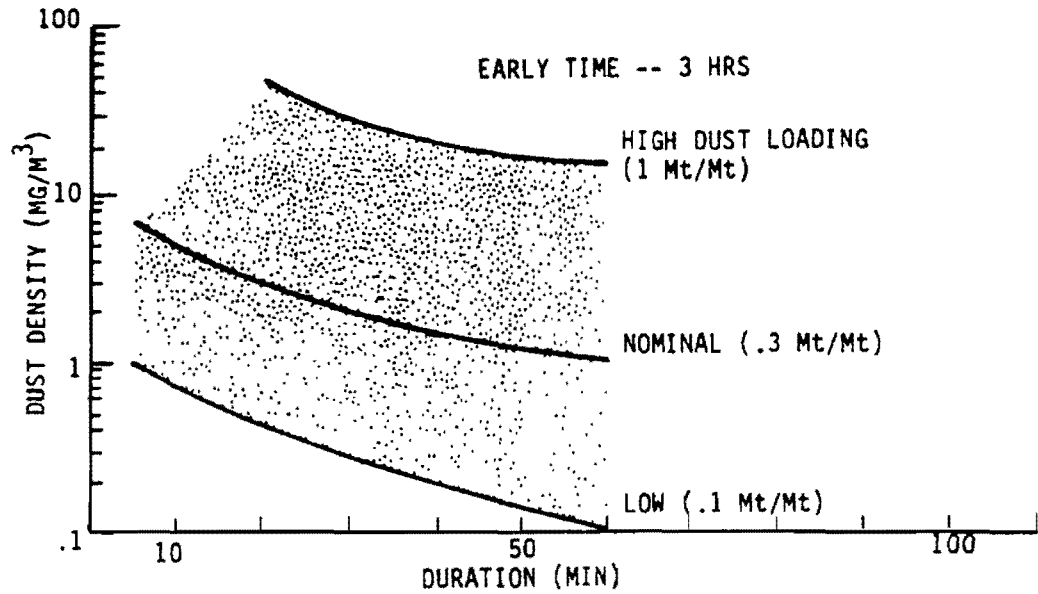


Figure 15. (U) Dust density vs duration of encounter.

# UNCLASSIFIED

encountered density levels resulting from uncertainties in the dust-loading factor. At early times, the flight path could pass through a maximum density of  $50 \text{ mg/m}^3$  for a total of 20 minutes and through  $15 \text{ mg/m}^3$  for a total of 60 minutes. At late times, the flight path could pass through a maximum of  $15 \text{ mg/m}^3$  for a total of 50 minutes and  $3 \text{ mg/m}^3$  for a total of 120 minutes. Excluding the  $3 \text{ mg/m}^3$  environment, all these conditions posit about the same total amount of dust encountered by an aircraft, 10 to  $12 \text{ kg/m}^2$  of intake area.

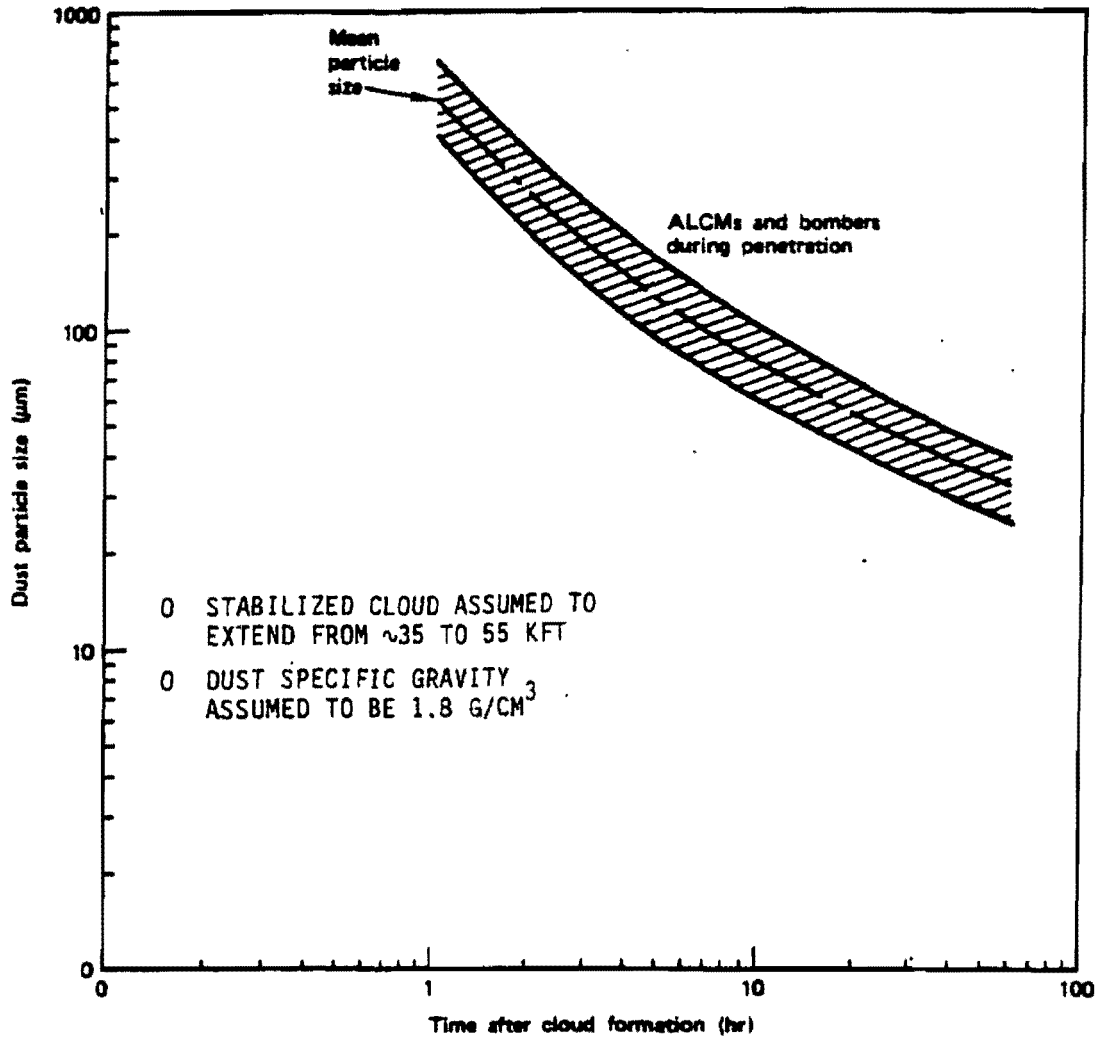
#### 4.4 (U) PARTICLE SIZE RANGE.

(U) Since ALCMs penetrate at very low altitudes, the dust particles they would encounter would be raining from the main cloud. Figure 16 shows, as a function of postdetonation time, the range of particle sizes that would be encountered near the ground (assumed to be sea level), having fallen from a cloud stabilized at 35 to 55 kft. At three hours postattack, the size range is predicted to be about 120 to  $250 \mu\text{m}$ ; at ten hours postattack, this decreases to a range of about 60 to  $110 \mu\text{m}$ .

#### 4.5 (U) SOVIET SOILS: DUST COMPOSITION FOR THE F-107 TESTS.

(U) Available references indicate that the characteristics of the soils surrounding major Soviet targets are generally similar to soil in the Great Plains region of the United States. In response to strong interest in early testing of the F-107 engine, we recommended for the testing of these engines a mixture that consisted of available soil from Warren AFB, Wyoming, combined with Mount St. Helens ash to simulate the composition of dust clouds that might be

UNCLASSIFIED



UNCLASSIFIED

Figure 16. (U) Particle size range near the ground.

UNCLASSIFIED

# UNCLASSIFIED

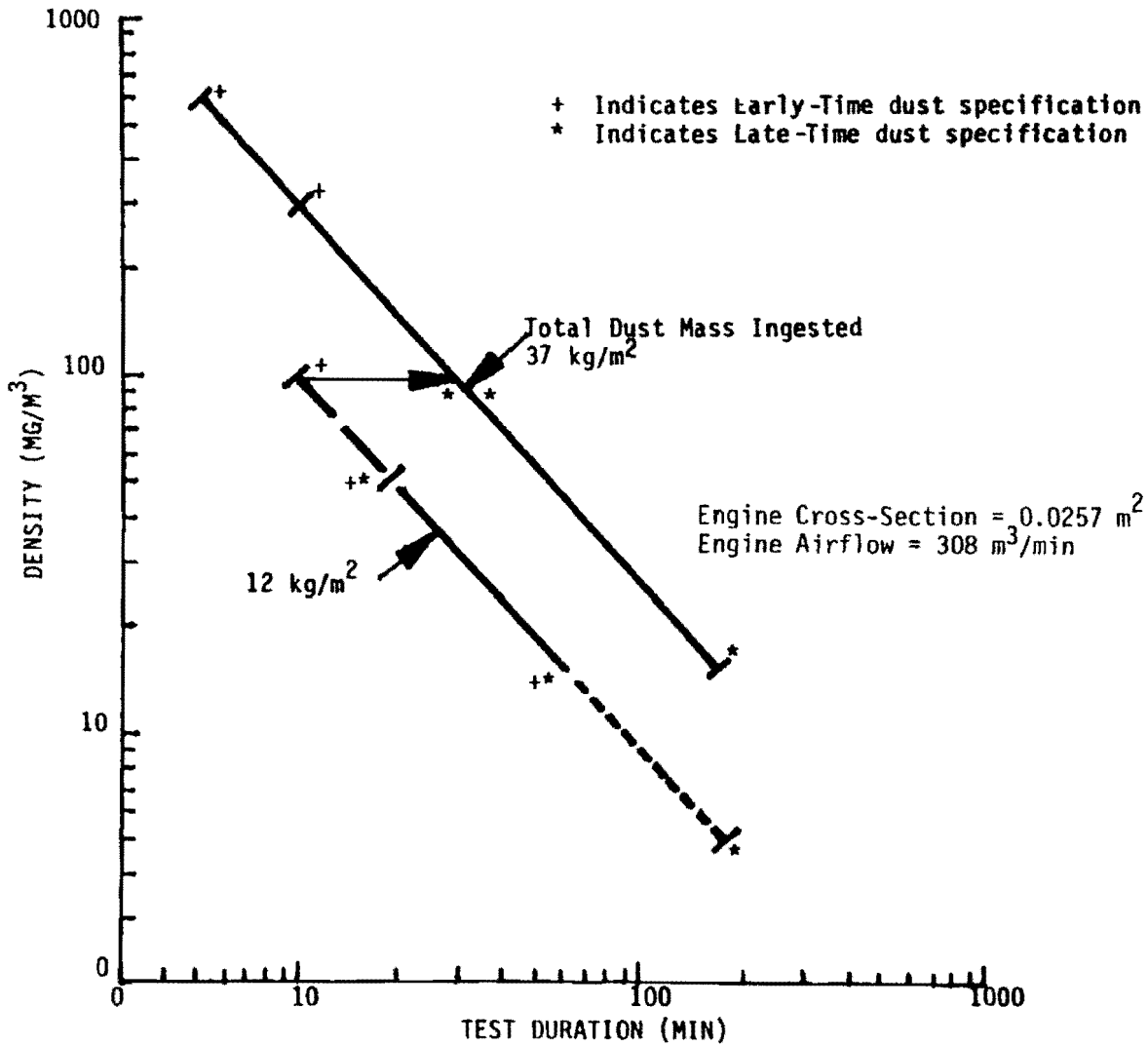
encountered by an ALCM. The Mount St. Helens ash was used as a source of glass because its chemistry is similar to typical midcontinent soils. It was mixed in a proportion to provide the glass fraction discussed in Section 3.5.3.

## 4.6 (U) SUMMARY OF TEST CONDITIONS.

(U) Figure 17 shows the suggested envelope of test points. The lower line, which represents a total ingested dust mass of  $12 \text{ kg/m}^2$ , follows directly from the results presented in Section 4.3.

(U) As stated previously, our dust environment estimates neglect the effects of particle agglomeration and the contributions of the dust stem and pedestal. Furthermore, some of the SIOP type of nuclear attack scenarios developed for planning purposes contain more surface bursts than does the SABRE ENDURE scenario used in making the estimates presented in this section. For these reasons, we assumed an upper bound on the dust environments that is a factor of 3 higher than our nominal estimates. This is illustrated in Figure 17, in which the lower line is extended to include the point at  $100 \text{ mg/m}^3$  density and the upper bound line represents a total ingested dust mass of  $37 \text{ kg/m}^2$ .

(U) Table 4 shows the suggested characteristics of the test materials. Two separate sets of composition and particle size range are used to represent the low-altitude early-time (3 to 10 hours) and late-time (>10 hours) dust environment.



UNCLASSIFIED

Figure 17 (U) Suggested test envelope.

# UNCLASSIFIED

Table 4. (U) Suggested test materials.

UNCLASSIFIED

Parameters	Early Times	Late Times
Dust composition	1 part ash 1 part clay soil <sup>1</sup> 1 part sandy soil <sup>1</sup>	2 parts ash 1 part clay soil <sup>1</sup>
Particle size range	63 to 250 $\mu\text{m}$ (dry sieved)	38 to 106 $\mu\text{m}$ (dry sieved)
Particle size distribution <sup>2</sup>	R <sup>-3.7</sup>	R <sup>-3.7</sup>

<sup>1</sup> (U) Soils taken from site of F.E. Warren Air Force Base.

<sup>2</sup> (U) R = particle radius.

UNCLASSIFIED

**UNCLASSIFIED**

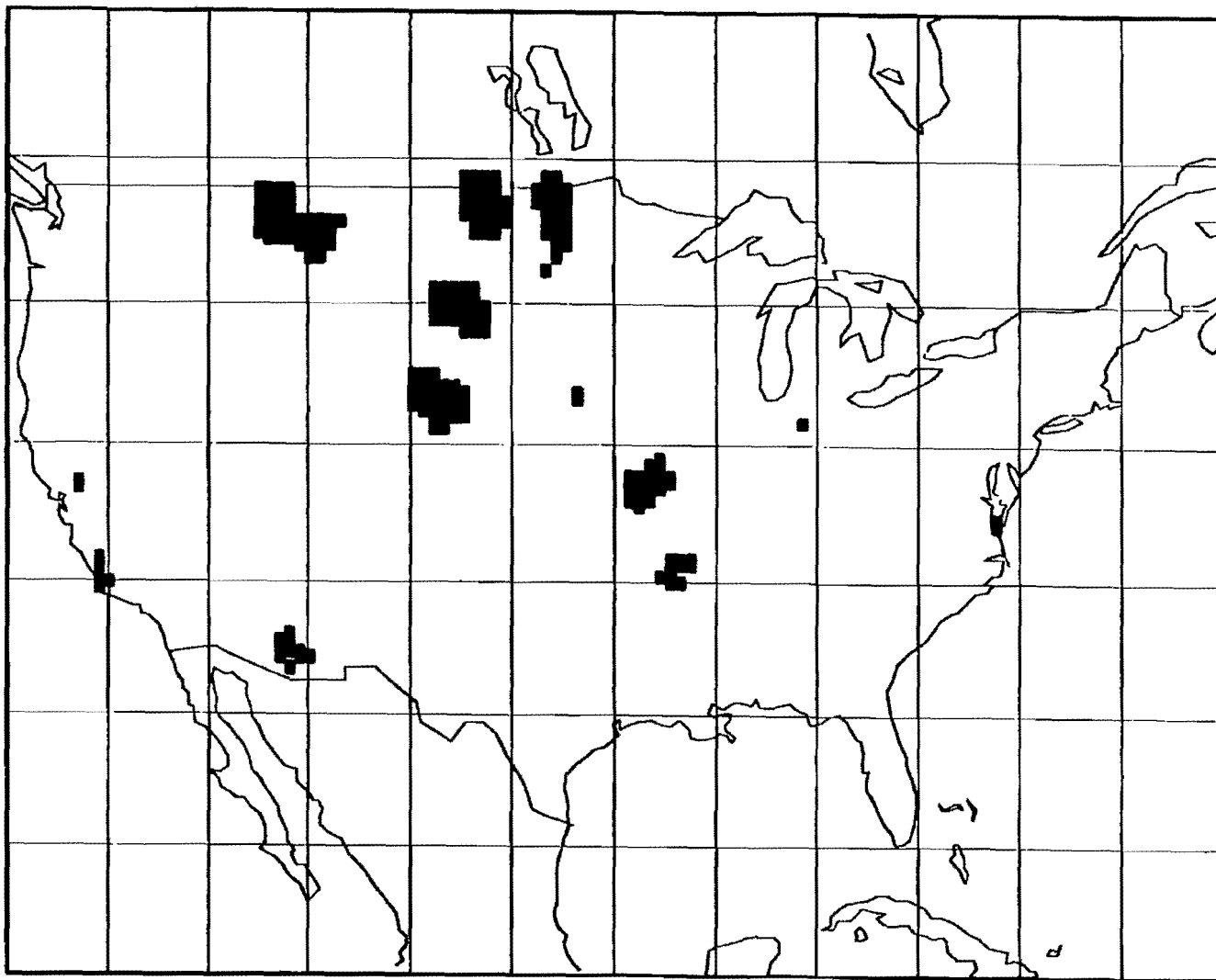
**THIS PAGE IS INTENTIONALLY LEFT BLANK.**

**UNCLASSIFIED**

*Pages 49 through 60  
are deleted.*

UNCLASSIFIED

51



UNCLASSIFIED

UNCLASSIFIED

Figure 18. (U) Stabilized clouds from the modified PRIZE GAUNTLET scenario.

# UNCLASSIFIED

Table 6. (U) Characteristics of the alternative laydown on CONUS.

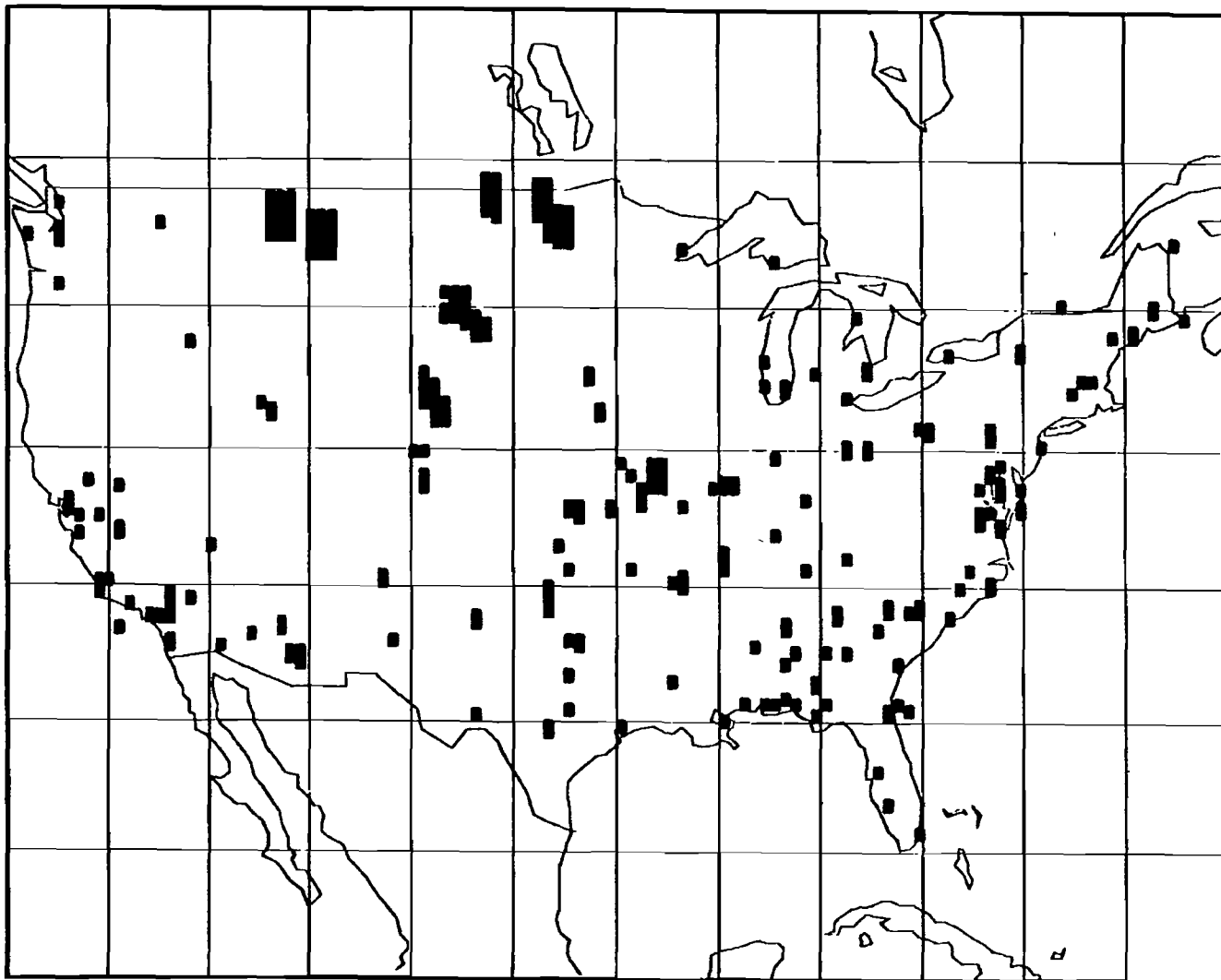
UNCLASSIFIED

- Uses only 0.5 and 1 MT yields.
- Ignores non-dust-creating bursts
- Has 1160 missile-related aim points.  
Has 250 other military aim points.
- Uses the following weapons:
  - Case 1: 3450 weapons of 0.5 MT  
100 weapons of mixed 1 and 0.5 MT
  - Case 2: 3450 weapons of 0.5 MT  
420 weapons of mixed 1 and 0.5 MT

UNCLASSIFIED

UNCLASSIFIED

54



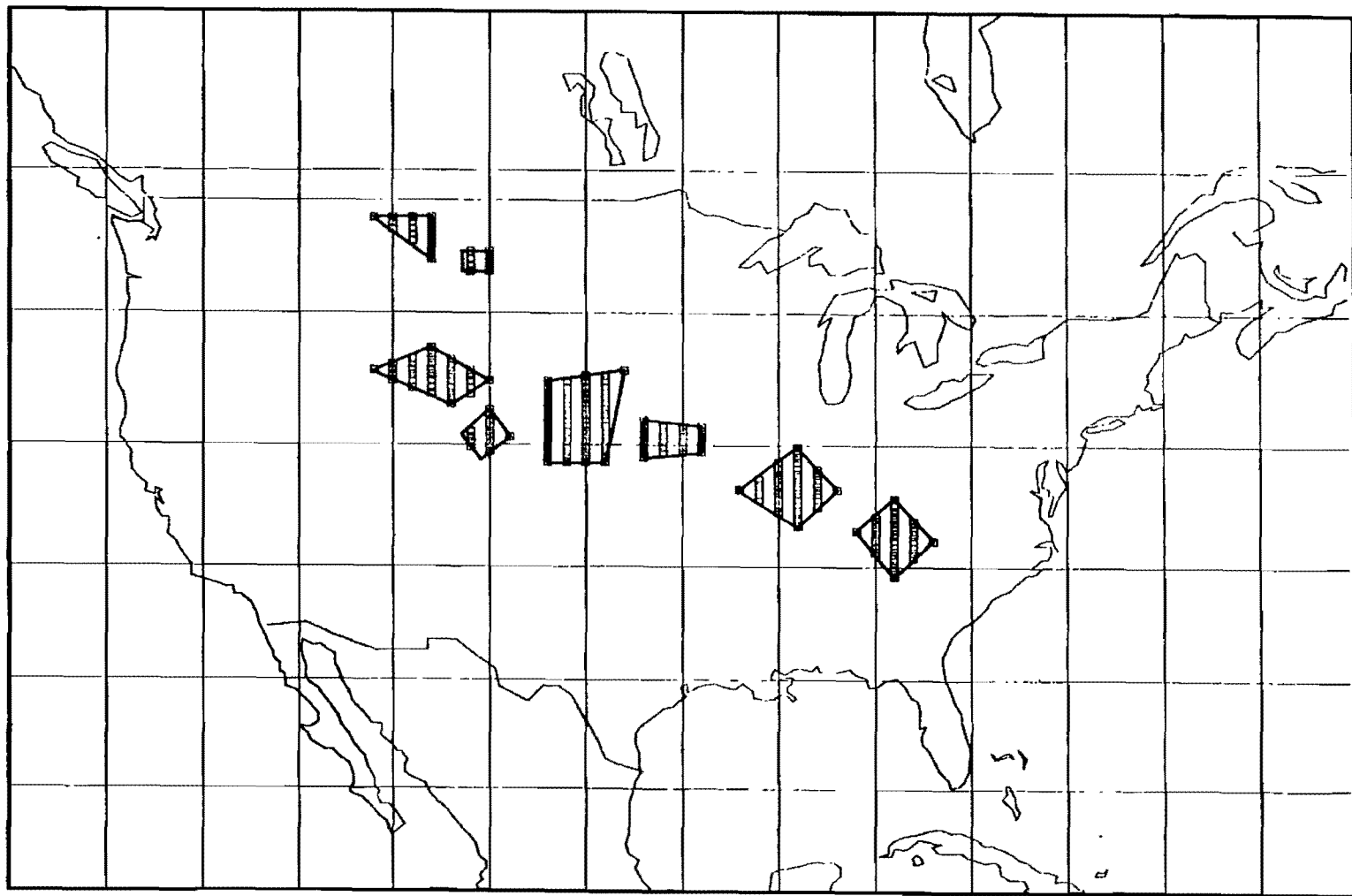
UNCLASSIFIED

Figure 19. (U) Stabilized clouds from the alternative laydown on CONUS.

UNCLASSIFIED

UNCLASSIFIED

56



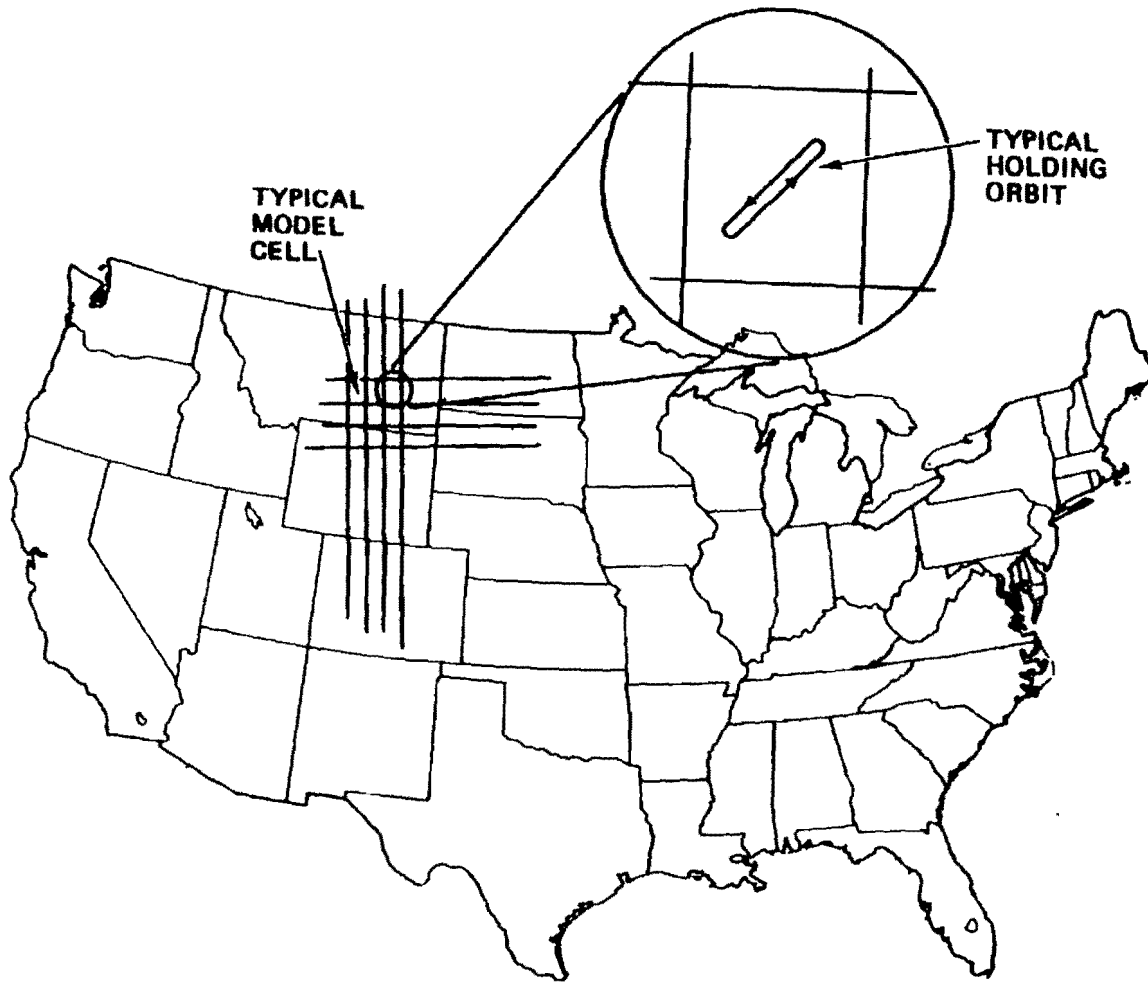
UNCLASSIFIED

UNCLASSIFIED

Figure 20. (U) Example of PACCS station areas.

UNCLASSIFIED

57



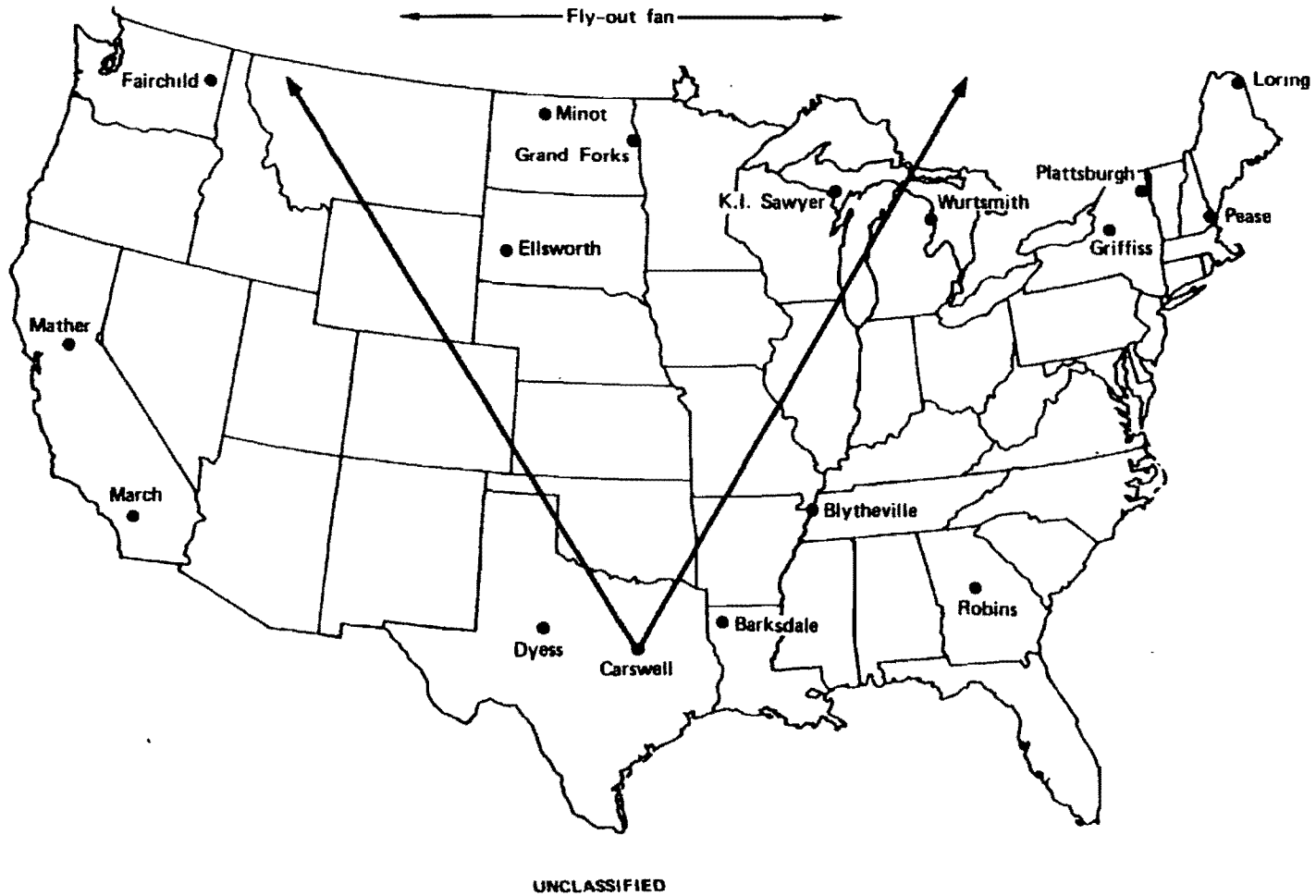
UNCLASSIFIED

UNCLASSIFIED

Figure 21. (U) Hypothetical PACCS orbits covering CONUS.

UNCLASSIFIED

59



UNCLASSIFIED

Figure 22. (U) Hypothetical bomber flight paths.

# UNCLASSIFIED

Table 7. (U) Summary of parameter excursions and their impact on the resulting dust environment.

UNCLASSIFIED		
Nominal case		
Early time (0.5 to 6.5 h)		100 kg/m <sup>2</sup>
Late time (12 to 18 h)		40 kg/m <sup>2</sup>
Parameter varied (nominal to excursion)	Effect on dust environment (relative to nominal case)	
<b>Mass lofted</b>		
1/3 MT/MT to 1 MT/MT		x3
1/3 MT/MT to 0.1 MT/MT		+3
Cloud stabilization altitudes (below to inside)		x2
Laydown yields 1 MT/m <sup>2</sup> to 2 MT/m <sup>2</sup>		x2
Worst location 99% to 100% in CONUS		x2
Particle size distribution (biased toward larger sizes)		+2
A/C entry time 0 to 0.5 h		1
Laydown	PRIZE GAUNTLET	1
	"Alternative laydown"	
	all NUDETs HOB=0	1
Winds	winter to summer	+1.2
Net factor		
	Up	Down
	x5.0	x0.4

## UNCLASSIFIED

(U) To explore the scenario sensitivity of dust environment estimates, we compared the results of the two laydowns described in Section 5.1. We also considered the effect of doubling the yield of ground bursts from 1 MT to 2 MT at each Missile Weapon System (MWS) aimpoint.

(U) We considered the following stabilized cloud parameter excursions. For dust-loading factors, excursions from the nominal loading of 1/3 MT/MT included the possible extremes of 0.1 and 1.0 MT/MT. Two different estimates of the particle size distribution were used: that inferred from JOHNNIE BOY data, and an excursion biased towards coarse particles (see Fig. 5). Because the clouds from many of the bursts in our scenarios stabilize near typical bomber and C<sup>3</sup> aircraft flight altitudes, we varied the base altitude of the cloud so that in one case the aircraft was below the cloud and in the other case the aircraft was within the stabilized cloud.

(U) In addition to these excursions, we compared the effects of average summer and winter winds. As will be shown later, although the actual location of the dust clouds varies with wind pattern, the areal extent and duration of dense dust regions and the maximum dust densities at any given post-attack time are relatively insensitive to our choice of winds.

(U) Since the clouds diffuse and are transported by winds and material falls out, the dust densities, spatial extent, and particle size distribution of the clouds encountered by aircraft depend on the age of the clouds, i.e., time elapsed since detonation. Cloud age at the time of encounter is particularly important to the PACCS aircraft and depends on

# UNCLASSIFIED

the force location at the time of attack. We considered two different possibilities. We assumed in one case that PACCS aircraft are on station at the time the detonation occurs, and thus allowed for the possibility that the aircraft interact with the very dense, newly formed clouds. In the other case, we assumed a 0.5-hour delay (attributable to the aircraft flight time to its station) before interaction might occur.

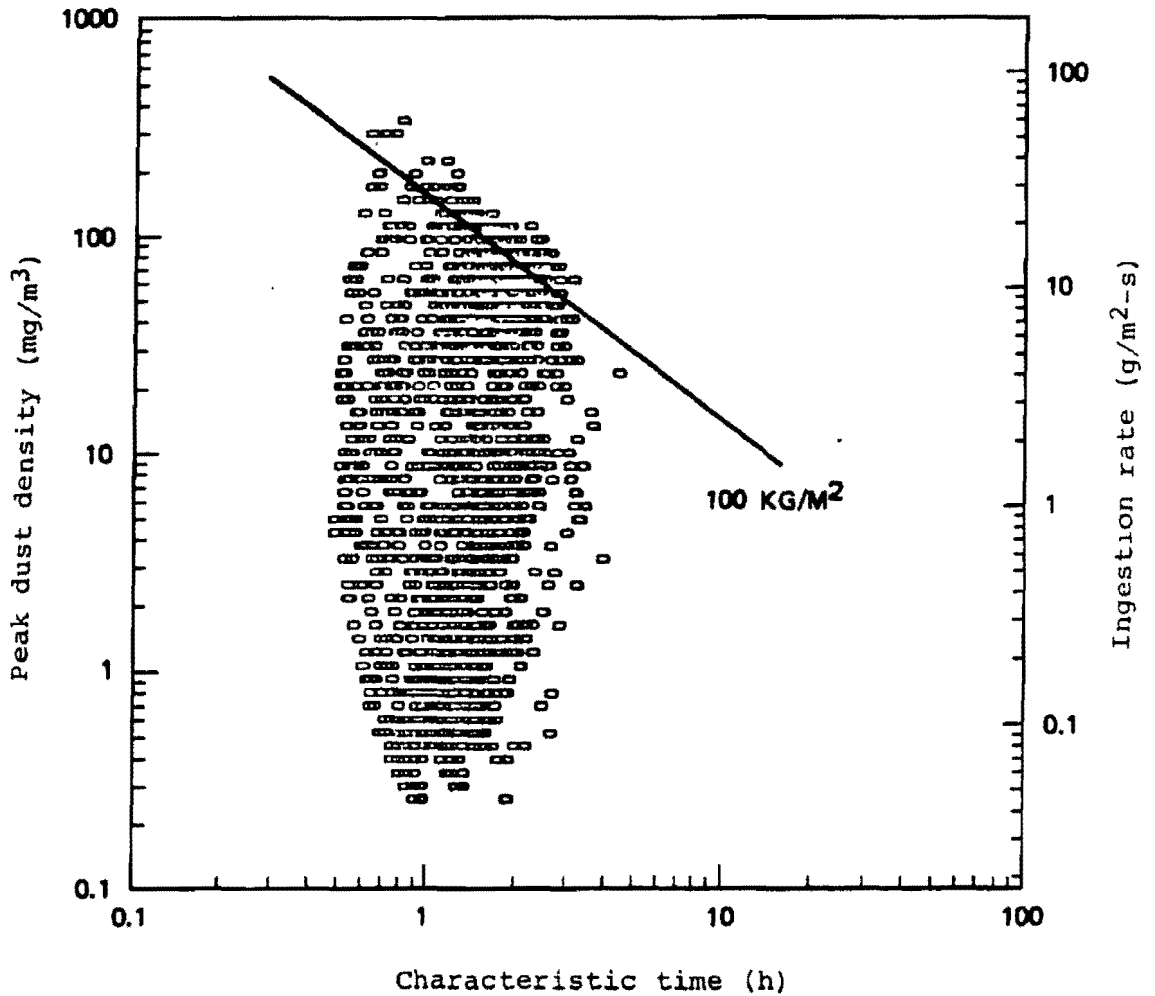
(U) The final input quantities listed in Table 1 relate to the dust model grid size. The vertical resolution is set at 10 kft. Its effect on the calculations has not been studied; but this interval, although a bit large, is not at great variance with the accuracy of other input quantities. The geographic spacing (which, as noted previously, is about 15 mi north-south, and 30 mi east-west) is large compared to the size of a single 1-MT dust cloud; for widely separated bursts, such spacing will result in an underestimate of the dust density, since the model conserves the dust mass but spreads it out over one model cell. On the other hand, this cell size is small compared to the size of a Minuteman field; thus, for these large multiple-targeted areas, inaccuracies in the description of individual detonations tend to be averaged out. This feature is important since the most stressing environments occur over these regions.

## 5.4 (U) RESULTS FOR PACCS AND B-52S.

### 5.4.1 (U) Results for PACCS.

(U) Our results on peak dust densities versus characteristic exposure times for the potential orbit positions in Figure 21 are displayed in Figures 23 (early-time encounters) and 24

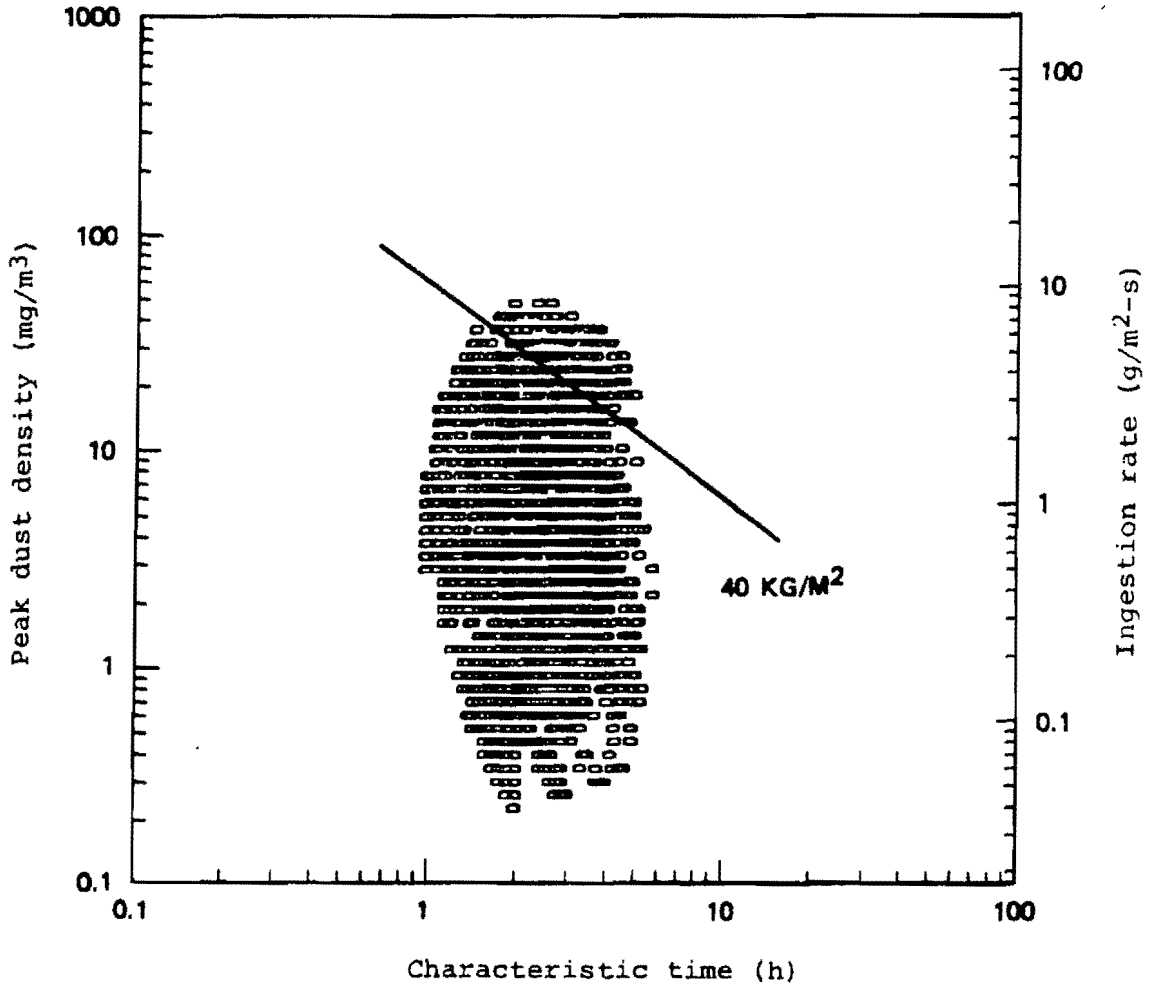
UNCLASSIFIED



UNCLASSIFIED

Figure 23. (U) Nominal peak dust density vs. encounter duration for PACCS aircraft--early times.

# UNCLASSIFIED



UNCLASSIFIED

Figure 24. (U) Nominal peak dust density vs. encounter duration for PACCS aircraft--late times.

# UNCLASSIFIED

(late-time encounters). Each point in the plots represents a single grid cell within CONUS that contains dust. The figures also show the peak ingestion rate, which is directly proportional to the peak density for a given assumed flight speed. The figures are based on the following set of nominal input parameters:

- An early-time period of 0.5 to 6.5 hours
- A late-time period of 12 to 18 hours
- A lofting efficiency of 1/3 MT/MT
- Flight below the cloud bottom
- A 1-MT surface burst targeted at each MWS aimpoint
- The JOHNNIE BOY particle size distribution
- Summer winds

(U) Figure 23 shows that the upper bound on the plot of density versus exposure time corresponds roughly to a total ingested mass of  $100 \text{ kg/m}^2$ . This  $100\text{-kg/m}^2$  line lies above the results for 99 percent of the cells covering CONUS. Thus, only 1 percent of the orbit positions will result in intercepted dust masses of more than  $100 \text{ kg/m}^2$ . The corresponding 99-percentile estimate for the ingested mass during the late period (Fig. 24) is about  $40 \text{ kg/m}^2$ .

#### 5.4.2 (U) Results for B-52s.

(U) Figure 25 displays similar results for the set of nominal environments that B-52s flying from southern CONUS bases may have to fly through. Note that there are far fewer points available than for the PACCS study, since only a few flyouts were sampled. The 99-percentile value of the total ingested mass is about  $30 \text{ kg/m}^2$ , which is a factor of

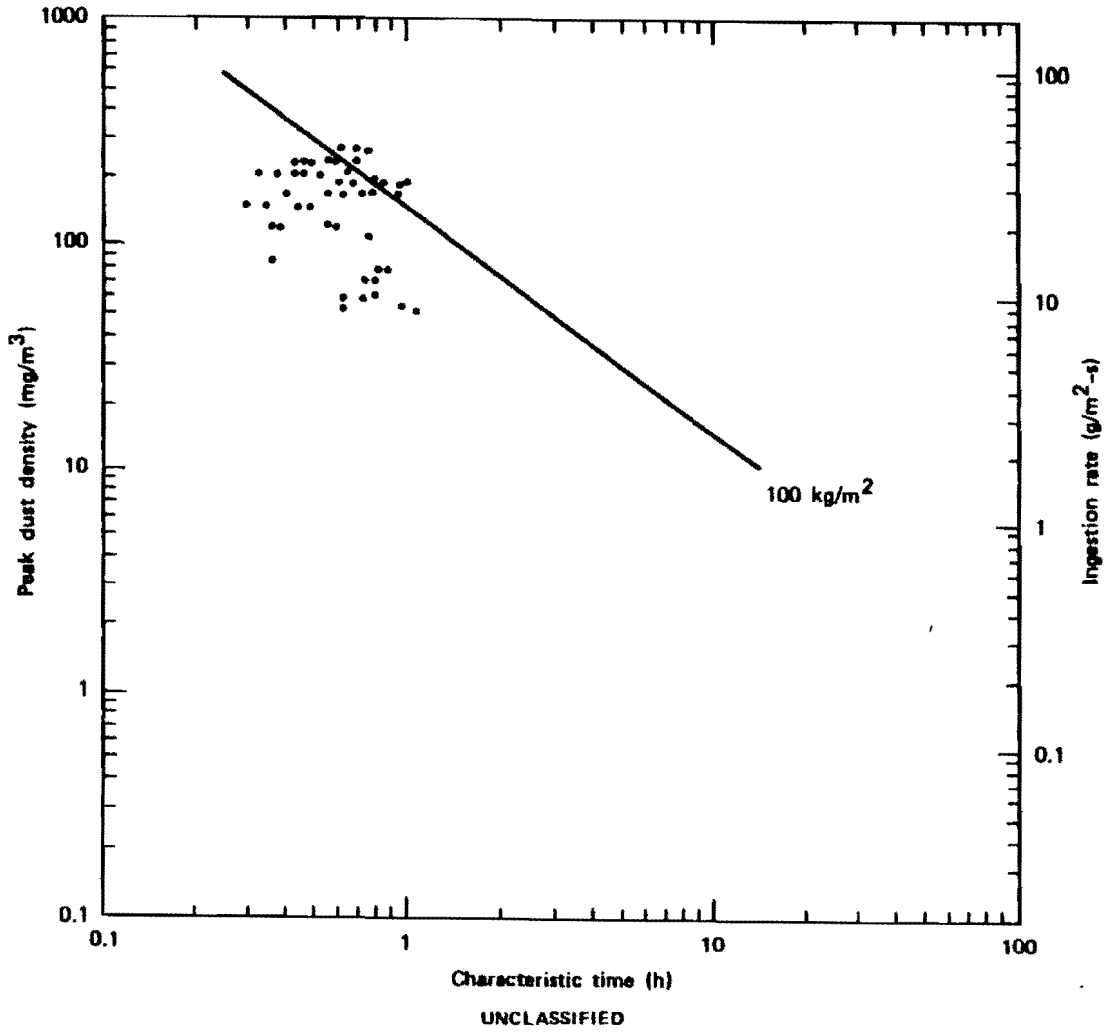


Figure 25. (U) Peak density vs. encounter duration for bomber and tanker flyouts.

## UNCLASSIFIED

about 3 less severe than the nominal early-time PACCS environment. The bombers and tankers are assumed to be operating in the same dust clouds as the PACCS aircraft so the peak densities are about the same. However, the bomber and tanker engines ingest less dust than those of the PACCS aircraft because they fly straight through the environment, whereas the PACCS aircraft must orbit for extended periods of time in a potentially dusty environment. The recommended engine test conditions are based on the severer environments predicted for the PACCS aircraft.

### 5.5 (U) RADIATION EXPOSURE CONSTRAINTS.

(U) In addition to possible mechanical damage to an aircraft's engines caused by dust ingestion, exposure of the air crew to radioactivity carried by the dust particles also jeopardizes their ability to carry out their mission. This section addresses the limits on dust quantities, and therefore on engine test conditions, imposed by radiation dose levels that of themselves prevent mission completion.

(U) The amount of radioactivity per unit of mass varies with particle size. Also, unlike particle mass, the amount of radioactivity decays with time. Thus, a particular dust density would correspond to higher dose rates at earlier times and lower dose rates at later times--the latter being more appropriate to consider for the purpose of this report, since it will give an upper bound on the dust environment.

(U) To find the bounds imposed on the test dust environments by the crew's tolerance to radiation, we estimated the total accumulated doses associated with the dust

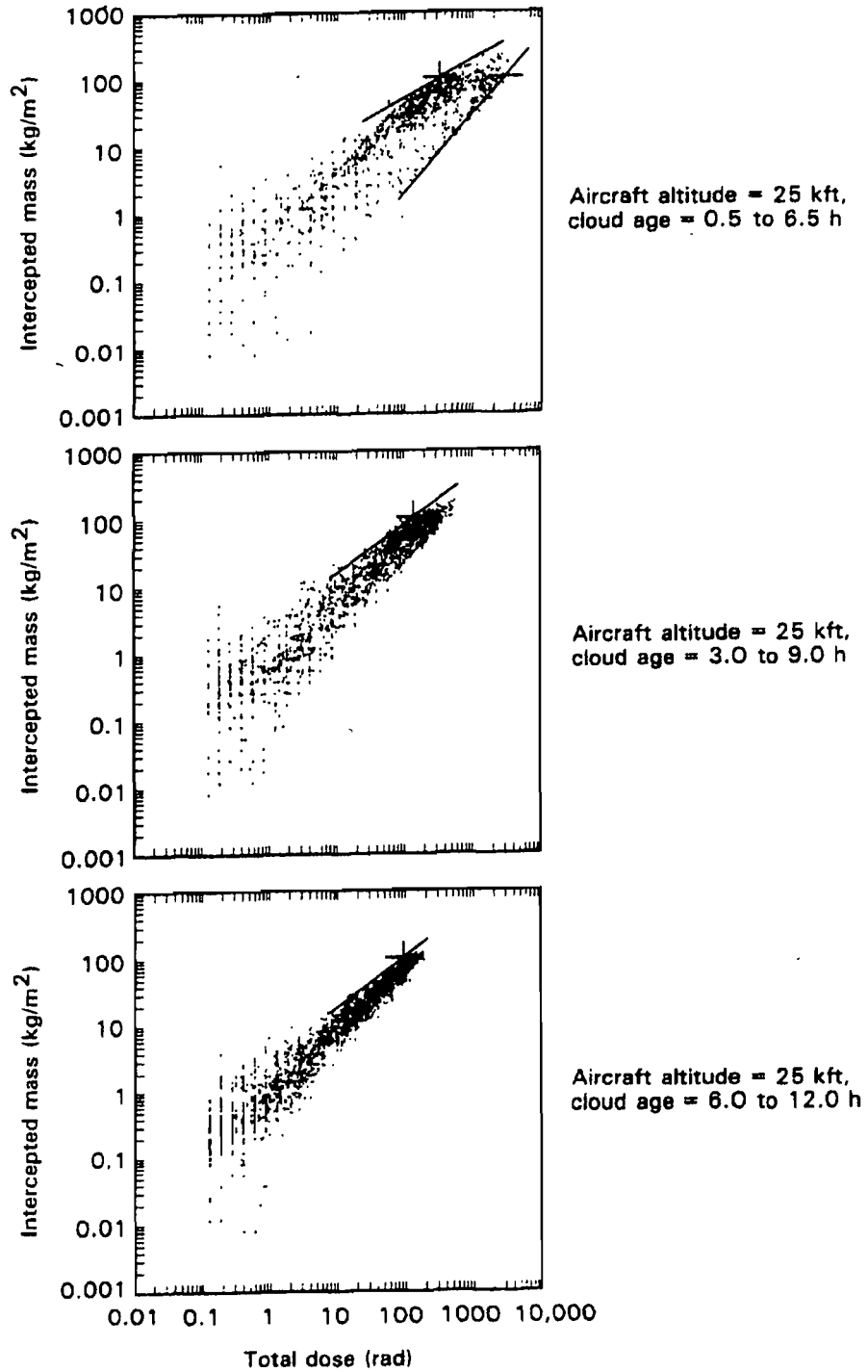
## UNCLASSIFIED

environments estimates presented above. The results are displayed in the scatter plots shown in Figures 26 and 27. We only considered environments for the PACCS aircraft, since the dust environments (and therefore the radiation hazard) have been shown to be more stressing for the PACCS aircraft than for the bombers.

(U) Figures 26 and 27 show, respectively, plots of total intercepted mass (accumulated over a 6-hour duration) versus total dose and plots of peak dust density versus total dose for the nominal model inputs discussed in Section 5.4.2 and a fission fraction of 0.8. Results are shown for three different cloud entry times: 0.5 hours, 3 hours, and 6 hours post-attack. The points in the plots correspond to the dust and radiation environments estimated for the hypothetical orbits of Figure 21.

(U) It may be seen from Figure 26 that the radiation dose varies between 100 and 3000 rads for the nominal maximum dust mass of  $100 \text{ kg/m}^2$  estimated previously for the PACCS orbits. This lower value is considerably less than the doses that would prevent the aircrews from completing their missions. Therefore, we conclude that even dust environments as severe as the 99-percentile environment (predicted for the nominal model inputs) do not impose a radiation hazard that will jeopardize the crews' ability to fulfill their missions. Furthermore, the input excursions that we defined in Section 5.4.2 to bound the effect of uncertainties in the input parameters on the dust environment estimates, or a reduction in the assumed fission fraction, would all tend either to increase the amount of ingested dust and radiation dose in the same proportion or to increase the ingested dust at a higher rate. Thus, we conclude that the upper bounds of

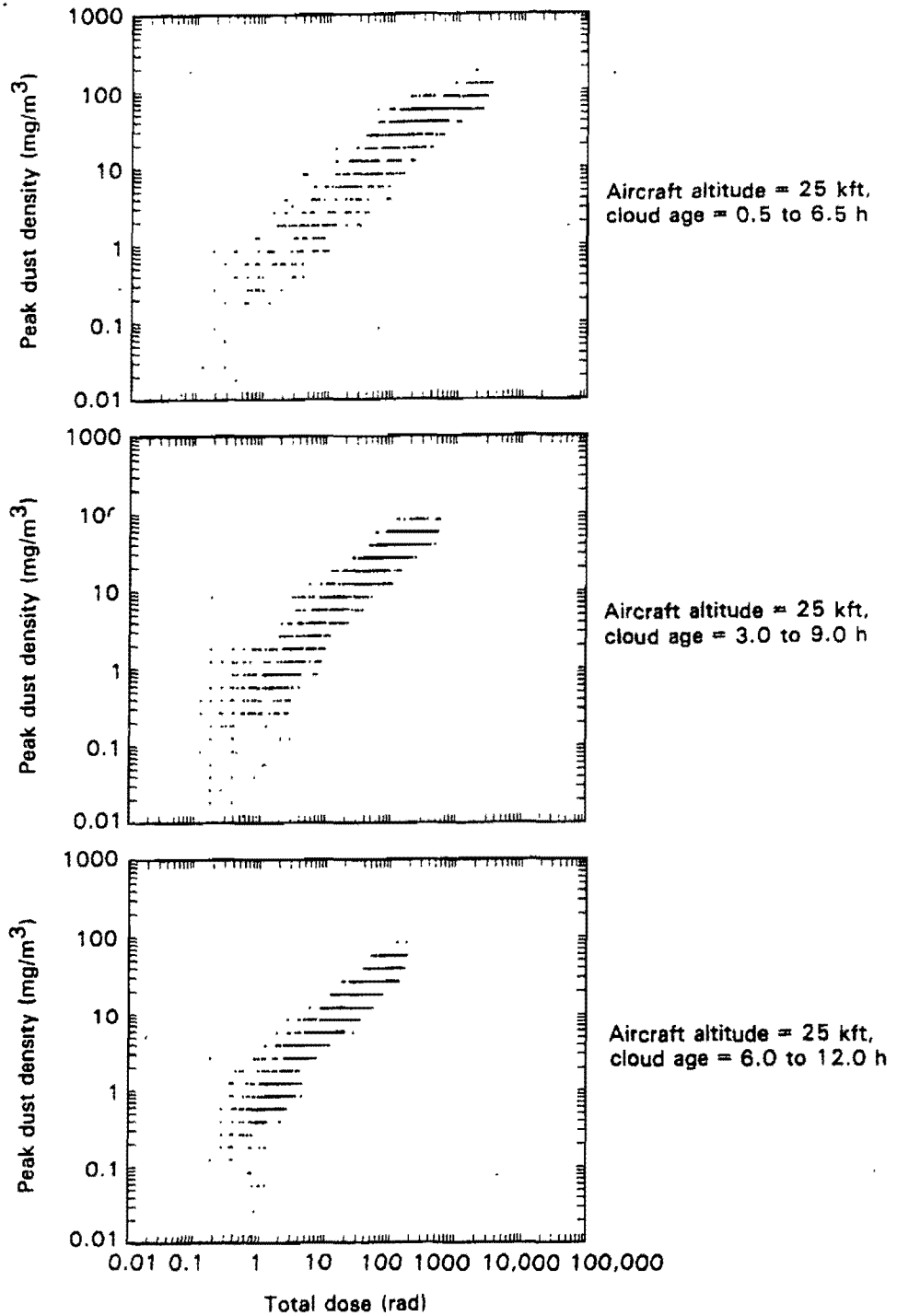
# UNCLASSIFIED



UNCLASSIFIED

Figure 26. (U) Radiation levels vs. total intercepted dust mass for nominal PACCS environments.

# UNCLASSIFIED



UNCLASSIFIED

Figure 27. (U) Radiation levels vs. peak dust density for nominal PACCS environments.

# UNCLASSIFIED

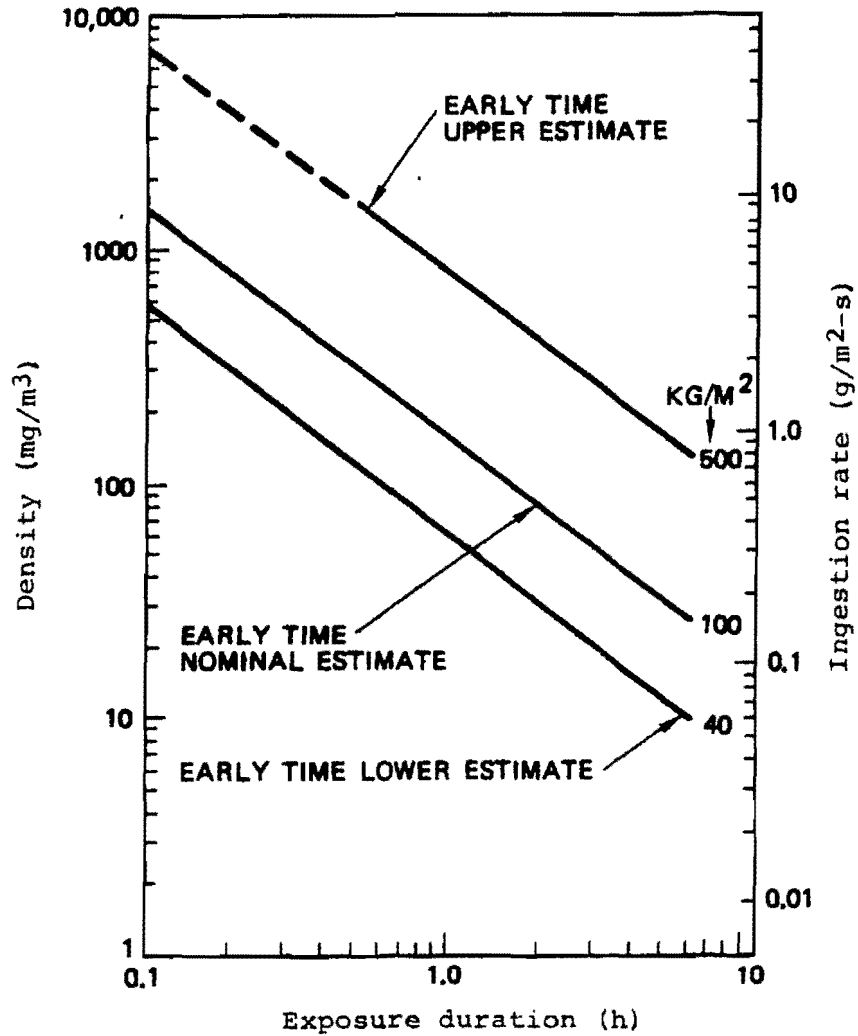
the engine test conditions should not be limited because of the radiation hazard to the crew.

## 5.6 (U) SUMMARY OF TEST CONDITIONS.

(U) Figure 28 shows the suggested test envelope of dust density versus exposure duration for the TF-33 and J-57 engines. This figure was based on the upper and lower bounds for the early-time PACCS results. (We did not consider the late-time PACCS results since that case produced less stressing environments.) The bounds were determined from Table 7 and the statistical procedure outlined in Section 5.3. The upper-limit estimate is a factor of 5 times the nominal result of  $100 \text{ kg/m}^2$  described in Section 5.4.2, or  $500 \text{ kg/m}^2$ . The lower bound on the environment is a factor of 0.4 times the nominal, or  $40 \text{ kg/m}^2$ .

(U) Table 8 shows the suggested composition of the test material. We chose only a single blend designed to be representative of the early-time (<6 hours) environment. The particle size distribution of this mixture is shown in Figure 29.

# UNCLASSIFIED



UNCLASSIFIED

Figure 28. (U) Suggested test envelope--upper and lower bounds on the dust environments for PACCS aircraft.

Table 8. (U) Suggested screening and mixing specifications for Calspan (dust composite preparation for engine tests of the generic CONUS environment).

UNCLASSIFIED

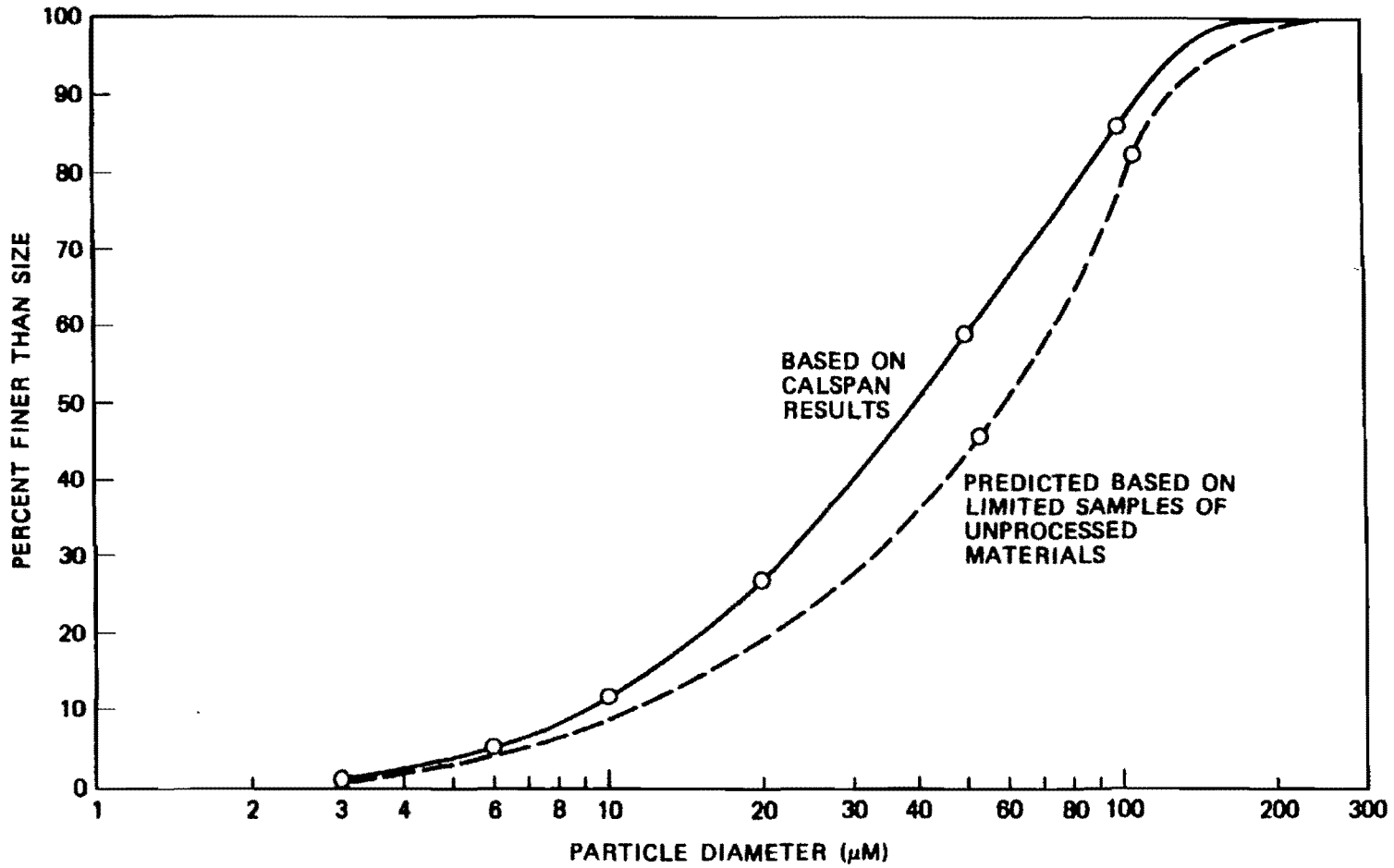
RECOMMENDED BLENDING PROPORTIONS	COMPOSITE COMPONENTS	SIZE BINS (PERCENTAGES BY WEIGHT OR VOLUME)					
		< 53 μM		53 - 106 μM		106 - 250 μM	
3/9	HOLLYWOOD SAND	25	+	50	+	25	= 100
2.5/9	CORONA CLAY	50	+	30	+	20	= 100
3/9	MT. ST. HELENS ASH (PORTLAND)	60	+	30	+	10	= 100
0.5/9	WYOMING BENTONITE	70	+	30	+	0	= 100
BLENDED COMPOSITE DUST		46	+	37	+	17	= 100

UNCLASSIFIED

73

UNCLASSIFIED

UNCLASSIFIED  
74



UNCLASSIFIED

Figure 29. (U) Particle size distribution of recommended CONUS environment composite.

# UNCLASSIFIED

## SECTION 6

### LIST OF REFERENCES

(This List Is Unclassified)

1. C.B. Gabbard, F. Perry, and R. Lelevier, Mt. St. Helens C-130 Encounter (U), DNA-TR-82-18, Defense Nuclear Agency, Washington, D.C., March 1982 (Confidential).
2. F.W. Perry/R&D Associates-Europe, letter to P. Rausch/R&D Associates-Marina, "Investigation of Aircraft Engine Ingestion of Volcanic Dust (Galunggung Eruptions June/July 1982)" (U), July 1982 (Unclassified).
3. P. Rausch, RDA technical note on Engine Dust Ingestion Issues, R&D Associates, Marina del Rey, CA, 1983 (Confidential).
4. M. Grover, B. Yoon, G. Willensky, and D. Yoon, A Sensitivity Study for Airborne Dust and Radiation Environment Modeling (U), DNA-TR-85-231, R&D Associates, Marina del Rey, CA, April 1985 (Secret).
5. H.J. Carpenter/R&D Associates-Marina del Rey, letter to E. Sevin et al./DNA, "Mass of Lofted Dust (U)," December 1982 (Unclassified).
6. G. Rawson, "Mass of Dust Lofted--Data Base Update (U)," interoffice correspondence, R&D Associates, Marina del Rey, CA, August, 1984 (Unclassified).
7. M. Rosenblatt et al., Nuclear Cloud Data Predictive Uncertainties (U), DNA 5508F, Defense Nuclear Agency, Washington, D.C., November 1980 (Secret).
8. M. Morgenthau et al., Local Fallout from Nuclear Test Detonations, Vol. II, Compilation of Fallout Patterns and Related Test Data (U), NDL-TR-34, DASA 1251, U.S. Army Nuclear Defense Laboratory, Edgewood Arsenal, MD, August 1963 (Secret-RD).
9. D.H. Sowle, Summary of Debris Altitudes Obtained from Satellite Data (U), MRC-R-243, Mission Research Corporation, Santa Barbara, CA, December 1985 (Secret).

# UNCLASSIFIED

## LIST OF REFERENCES (Concluded)

10. M.W. Nathans and R. Thews, The Particle Size Distribution of Nuclear Cloud Samples (U), Advances in Chemistry Series, No. 93, American Chemical Society, Washington, D.C., 1970 (Unclassified).
11. D. Cranmer/Aerospace, letter to G. Rawson/R&D Associates-Marina on characteristics of midcontinental soils, 2 August 1985 (Unclassified).
12. C. Ollier, Weathering, American Elsevier Publishing Company, Inc., New York, 1969 (Unclassified).
13. S-CUBED BM-3 Calculation, excerpts provided by J. Baker, S-CUBED, La Jolla, CA, May 1985 (Unclassified).
14. M. Rosenblatt and C. McArdle, "Single Burst Clouds," California Research and Technology, presented at DICE Environments for Fratricide Meeting, held at R&D Associates, Marina del Rey, CA, August 1985 (Unclassified).
15. M. Rosenblatt/CRT, personal communication to T. Mazzola/R&D Associates-Marina, July 1985 (Unclassified).
16. M. Rosenblatt, Critique of Our Capability to Calculate/Predict Nuclear Dust Clouds and Ejecta Fields (U), California Research and Technology, Chatsworth, CA, July 1982 (Secret-Formerly Restricted Data).

# UNCLASSIFIED

## DISTRIBUTION LIST

(This List Is Unclassified)

### DEPARTMENT OF DEFENSE

ASSISTANT TO THE SECRETARY OF DEFENSE  
ATOMIC ENERGY  
ATTN: EXECUTIVE ASSISTANT

DEFENSE INTELLIGENCE AGENCY  
ATTN: V FRATZKE  
2 CYS ATTN: RTS-2B

DEFENSE NUCLEAR AGENCY  
ATTN: SPWE  
4 CYS ATTN: TITL

DEFENSE NUCLEAR AGENCY  
ATTN: TDNM-CF  
ATTN: W SUMMA

DEFENSE TECH INFO CENTER  
2 CYS ATTN: DTIC/FDAB

JOINT STRAT TGT PLANNING STAFF  
ATTN: JK (ATTN: DNA REP)

LAWRENCE LIVERMORE NATIONAL LAB  
ATTN: DNA-LL

UNDER SECRETARY OF DEFENSE  
ATTN: LT COL R DAVIS  
ATTN: DIR CRUISE MISSILE SYS  
ATTN: LTC W RATHGABER  
ATTN: STRAT & THEATER NUC FORCES

### DEPARTMENT OF THE ARMY

AVIATION APPLIED TECHNOLOGY DIR  
ATTN: H MORROW  
ATTN: W SWINK

HARRY DIAMOND LABORATORIES  
ATTN: J GWALTNEY

U S ARMY AVIATION SYSTEMS CMD  
ATTN: LTC DEVAUGHAN

U S ARMY BALLISTIC RESEARCH LAB  
ATTN: S POLYAK  
ATTN: R RALEY

U S ARMY NUCLEAR & CHEM AGENCY  
ATTN: MONA-NU  
ATTN: MR LONG

### DEPARTMENT OF THE NAVY

NAVAL AIR SYSTEMS COMMAND  
ATTN: J ALDRIDGE

ATTN: MAJ HOLDSTEIN  
ATTN: PMA-274  
ATTN: PMA-275 V-22 DESK  
ATTN: LTC SHERWELL

NAVAL RESEARCH LABORATORY  
ATTN: CODE 2627 (TECH LIB)  
ATTN: D FORESTER

NAVAL WEAPONS CENTER  
ATTN: J MORROW

NAVAL WEAPONS EVAL FACILITY  
ATTN: CLASSIFIED LIBRARY  
ATTN: R TILLERY

OFC OF THE DEP CH OF NAVAL OPS  
ATTN: OP 654

### DEPARTMENT OF THE AIR FORCE

AERONAUTICAL SYSTEMS DIVISION  
ATTN: E PRICE  
ATTN: ASD/ENSS  
ATTN: H GRIFFIS  
ATTN: J DAY  
ATTN: ASD/YZWT

AIR FORCE CTR FOR STUDIES & ANALYSIS  
2 CYS ATTN: R GRIFFIN  
ATTN: AFCSA/SASB  
ATTN: MAJ TOM HOPKINS

AIR FORCE FLIGHT TEST CENTER  
ATTN: R HILDEBRAND

AIR FORCE OPNL TEST AND EVAL CTR  
ATTN: RD

AIR FORCE SYSTEMS COMMAND  
ATTN: DLAJ  
ATTN: DLWM  
ATTN: SDBC

AIR FORCE WEAPONS LABORATORY  
ATTN: A SHARP  
ATTN: E FRANKLIN  
ATTN: NTN(NGCS)  
ATTN: SUL

AIR FORCE WRIGHT AERONAUTICAL LAB  
ATTN: R DENISON

AIR FORCE WRIGHT AERONAUTICAL LAB  
2 CYS ATTN: W ANSPACH  
ATTN: M STIBICH

Dist-1

# UNCLASSIFIED

# UNCLASSIFIED

## DNA-TR-87-106 (DL CONTINUED)

AIR UNIVERSITY LIBRARY  
ATTN: AUL-LSE

DEPUTY CHIEF OF STAFF  
ATTN: AF/RDQM

DEPUTY CHIEF OF STAFF  
ATTN: RD L

STRATEGIC AIR COMMAND  
ATTN: XOBB  
ATTN: MAJ A PHILPOTTS

STRATEGIC AIR COMMAND  
ATTN: NRI/STINFO

STRATEGIC AIR COMMAND/XPFS  
ATTN: XRF5

**DEPARTMENT OF ENERGY**

SANDIA NATIONAL LABORATORIES  
ATTN: TECH LIB 3141

**OTHER GOVERNMENT**

CENTRAL INTELLIGENCE AGENCY  
ATTN: OSWR/NED

U S ARMS CONTROL & DISARMAMENT AGCY  
ATTN: H COOPER

**DEPARTMENT OF DEFENSE CONTRACTORS**

AEROSPACE CORP  
ATTN: H BLAES

BOEING CO  
ATTN: W SCHERER

BOEING HELICOPTERS  
ATTN: N CARAVASOS

CALSPAN CORP  
ATTN: C PADOVA  
ATTN: M DUNN

CARPENTER RESEARCH CORP  
ATTN: H J CARPENTER

DAMASKOS, INC  
ATTN: N DAMASKOS

DAYTON, UNIVERSITY OF  
ATTN: B WILT

GENERAL ELECTRIC CO  
ATTN: H BEUTEL  
ATTN: M SUD

GENERAL MOTORS CORPORATION  
ATTN: R YORK

GENERAL RESEARCH CORP  
ATTN: D MIHORA  
ATTN: R CRAWFORD  
ATTN: W ADLER

INSTITUTE FOR DEFENSE ANALYSES  
ATTN: E BAUER

IRT CORP  
ATTN: D WOODALL

KAMAN SCIENCES CORP  
ATTN: D COYNE  
ATTN: L MENTE  
ATTN: R RUETENIK  
ATTN: W LEE

KAMAN SCIENCES CORP  
ATTN: J SOVINSKY

KAMAN SCIENCES CORP  
ATTN: E CONRAD

KAMAN SCIENCES CORPORATION  
ATTN: DASIAC

KAMAN TEMPO  
ATTN: DASIAC

LOCKHEED AERONAUTICAL SYSTEMS  
ATTN: A SCHUETZ  
ATTN: B OSBORNE

LOCKHEED CORPORATION  
ATTN: R KELLY

MCDONNELL DOUGLAS CORP  
ATTN: H SAMS

MCDONNELL DOUGLAS CORP  
ATTN: J TRACY  
ATTN: L COHEN

MCDONNELL DOUGLAS CORP  
ATTN: J MCGREW  
ATTN: M POTTER

NORTHROP CORP  
ATTN: C GUADAGNINO

PACIFIC-SIERRA RESEARCH CORP  
ATTN: H BRODE

R & D ASSOCIATES  
2 CYS ATTN: B L YOON  
2 CYS ATTN: P RAUSCH  
2 CYS ATTN: R A GREENE  
2 CYS ATTN: T MAZZOLA

Dist-2

# UNCLASSIFIED

# UNCLASSIFIED

DNA-TR-87-106 (DL CONTINUED)

2 CYS ATTN: R RAWSON  
ATTN: T PUCIK

RAND CORP  
ATTN: B BENNETT

ROCKWELL INTERNATIONAL CORP  
ATTN: A MUSICMAN  
ATTN: P MASON

SCIENCE APPLICATIONS INTL CORP  
ATTN: J COCKAYNE

SCIENCE APPLICATIONS INTL CORP  
ATTN: A MARTELLUCCI

SOUTHERN RESEARCH INSTITUTE  
ATTN: C PEARS  
ATTN: S CAUSEY

SPARTA SYSTEMS, INC  
ATTN: J DUBEL

TOYON RESEARCH CORP  
ATTN: J CUNNINGHAM

UNITED TECHNOLOGIES CORP  
ATTN: R FOULKROD

UNITED TECHNOLOGIES CORP  
ATTN: J TARBOX

UNITED TECHNOLOGIES CORP  
ATTN: M TATUM

Dist-3

# UNCLASSIFIED

UNCLASSIFIED

THIS PAGE IS INTENTIONALLY LEFT BLANK.

Dist-4

UNCLASSIFIED

[REDACTED]

**UNCLASSIFIED**

[REDACTED]  
[REDACTED] to  
[REDACTED] ns  
Hand [REDACTED] gn  
dis [REDACTED] nic  
En [REDACTED]

**UNCLASSIFIED**  
[REDACTED]